Design and Implementation of Phase Difference Type Laser Range Finder

A Project Report

submitted by

C RAMANATHA RAVI TEJA

in partial fulfillment of the requirements

for the award of the degrees of

BACHELOR OF TECHNOLOGY

and

MASTER OF TECHNOLOGY

DEPARTMENT OF ELECTRICAL ENGINEERING

INDIAN INSTITUTE OF TECHNOLOGY MADRAS

JUNE 2011

THESIS CERTIFICATE

This is to certify that the thesis titled **Design and Implementation of Phase Difference Type Laser Range Finder** being submitted by **C. Ramanatha Raviteja (EE06B033)** to the **Indian Institute of Technology Madras** for the award of the degrees of **Bachelor of Technology** and **Master of Technology** is a bona fide record of the research work carried out by him in the Department of Electrical Engineering under my supervision. The contents of this thesis, in full or in parts, have not been submitted to any other University or Institute for the award of any degree or diploma.

Dr. Nagendra Krishnapura
Project Advisor
Assistant Professor
Department of Electrical Engineering
IIT Madras, 600036

Place: Chennai
Date: 12th June 2011

ACKNOWLEDGEMENTS

I would like to thank my project guide Dr. Nagendra from whom I learnt many essential qualities of a good engineer. His clarity in the fundamentals and the ‘no hand-waving’ approach are amazing. He definitely is my role model in that aspect. I would also like to express my gratitude to Anish Bekal, Mr. Nanda Kumar and Mr. Prabhakar Rao for the timely and practical help that they have provided when I was stuck in some parts of the project. I would like to thank Dr. Balaji Srinivasan, who introduced me to the wonderful world of EM waves and Photonics and showed many interesting demonstrations which increased my interest and curiosity in those fields. I would like to thank Dr. Harishankar Ramachandran for his CAD lab course. If it were not for that course I would not have been half as confident in MATLAB and C++ as I am now. I would like to thank Dr. V Jagadeesh Kumar for the insights that he provided me whenever I met him for help. I thank Dr. Shanti Pavan, Dr. Nandita Das Gupta, Dr. Arun Mahindrakar and Dr. Sridharan for teaching and support that they provided me.

I thank my friend Jitagna for the support that he had given me all through my activities in the Insti. I thank my friend Harshit for the great fellow that he had been and the way that he influenced my thinking. I thank Manikanta Avinash and Harish Ravishankar for the great discussions that we had. I thank my friends, J Square, Babloo, Unula, Raja, Peeche, Puneeth, Nampu, Sidepro, Branded, Virinchi, Parw, Quarter and Behen for the awesome experiences that they have given to me as wing mates. I am grateful to Aditya Chouksey for always doing assignments along with me just before the deadline. I thank my class people for the good class that they have made.

I thank Ravikanth, Subhash, Rohit, Vivek, Geography, Pavan Holla, Kedar, Bijli, Rigid, Prateek, Pranay Hem, Enba, Blade, Rajan, Satish, Pavan Rohit, Varun N, Himatej, Nagender, Shashank, Anish, Girish, Seshan and other CFI junta for the wonderful people that they have been. I thank the present Dean Students, Prof. M Govardhan, Ex- Dean Students, Prof. V G Idichandy, Dr. Prathap Haridoss and Dr. T S Natarajan for providing

me an excellent opportunity called Centre for Innovation. I thank Amrutash for working relentlessly for it.

Last but not the least, I want to thank my parents, Ramakrishna & Varalakshmi and my sister, Purnima for the way they brought me up to this level and taught me many things. I would like to dedicate this work of mine to my parents and my sister.

C Ramanatha Raviteja

20th June 2011

ABSTRACT

KEYWORDS: Laser Range Finder, Phase difference type Laser Range Finder, LIDAR

In this project, a system level design and implementation of a phase difference type Laser range finder has been presented. An intensity modulated Laser light is sent to the target. The light reflected from the target is detected using a photodiode and amplifier circuit. The phase difference between the transmitted light and the received light is directly proportional to the distance. This phase difference is measured and the distance is estimated. This distance is shown on a display in units of centimeter. The data can also be logged on a computer.

The design is implemented on a Printed Circuit board. The Laser Range finder made has a range of 0.5m to 1.8m and a resolution of 2mm. It can update the distance onto a computer at a rate of 600 samples per second. The accuracy of the Laser Range finder has been tested for white surfaces. The measured data, standard deviation of the measured data, accuracy and other parameters have been presented for the white screen target. Percentage error vs. actual distance graphs for four different colors are presented.

TABLE OF CONTENTS

LIST OF FIGURES

ABBREVIATIONS

LIDAR	Light Detection and Ranging
USB	Universal Serial Bus
PCB	Printed Circuit Board
APD	Avalanche Photo-diode
BPF	Band Pass Filter
TOF	Time of Flight
LASER	Light Amplification by Stimulated Emission of Radiation
PC	Personal Computer
SNR	Signal to Noise Ratio
NSD	Noise Spectral Density
SD	Standard Deviation
SMD	Surface Mount Device
EAGLE	Easily Applicable Graphical Layout Editor
SMA	Sub Miniature version A
ISP	In System Programming
USART	Universal Synchronous and Asynchronous Reception and Transmission

CHAPTER 1

Introduction

Laser Range Finding is an important method to measure distances between the sensor and the target. Being a non-contact way of measuring the distances makes it very handy in measurements. It was invented in early 1960s and found immediate applications in civil engineering for making measurements. Laser Range finding is also used in Terrain mapping, Laser altimeter, Atmospheric studies etc. The use of Laser Range finding in Robotics started more recently with increasing need for accurate and fast obstacle sensing in mobile robots. Laser Range finders are used on robots so as to enable the robots sense how far they are from obstacles in each direction. These Laser Range finders typically are designed for low range (few meters) and high resolution (few milli meters). There are Laser Range finders which can scan the environment and give a map of all the obstacles in horizontal plane. The high cost of these sensors is one of the main hindrances for ubiquitous use of these sensors. The high cost of these Laser Range finders and their increasing use in the field of Robotics was the main motivation behind the project.

This thesis explains, the design, implementation and testing of the Laser Range finder made. Before going into these details, a short introduction about two different kinds of Laser Range finding systems is presented.

1.1 Laser Range finding techniques

Two different kinds of Laser Range finders exist depending on the technique used for Laser Range finding. They are

- Time of Flight (TOF) type LIDAR (Light Detection and Ranging)
- Phase Difference type LIDAR

The principle of working, advantages and disadvantages of these Ranging methods are presented in the following sections.

1.1.1 Time of Flight type LIDAR

In this type of LIDAR, a very narrow light pulse is sent onto the target. This pulse of light falls on the target and gets reflected. The reflected light is received by the receiver and the time difference between the transmission and reception of the light pulse is measured. This time difference when multiplied by the speed of light and halved, gives the required distance. The principle is shown in the Fig. 1.1.

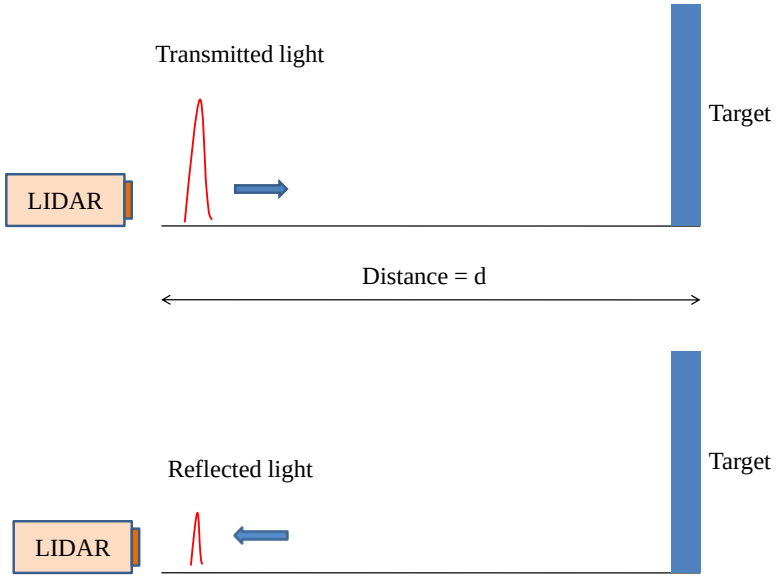

Fig. 1.1: Illustration of the principle of TOF type LIDAR.

The distance between the Range finder and the target is given by $ct/2$ where c is the speed of light in air and t is the time difference between the sent out light pulse and the received light pulse. One of the main advantages of the TOF type LIDAR is that the range is not bound except by the minimum threshold intensity required to detect the received signal. The main disadvantage of this method is that the pulse shape of both the transmitted light and the received light should be very narrow for high resolution in measuring distance. Due to the above advantages and limitations, this kind of LIDAR is

best suited for outdoor applications where the range required is large and the resolution requirement is less stringent.

1.1.2 Phase difference type LIDAR

In a Phase difference type of LIDAR, a modulated light wave (typically LASER light) is incident onto the target. The transmitted light and the reflected light have different phase as the modulated light accumulates phase on the path. This phase difference is directly proportional to the distance. By measuring the phase difference between both the light waves, the distance can be estimated. This technique is illustrated in Fig. 1.2.

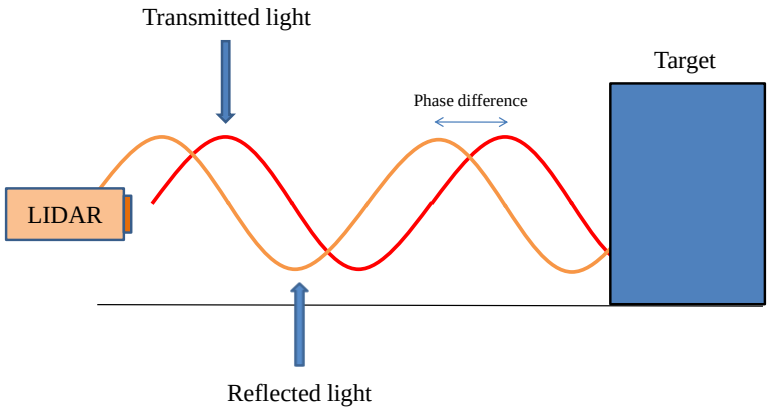

Fig. 1.2: Illustration of the principle of a Phase Difference type LIDAR.

In the above figure, the Red colour wave represents the transmitted light and the orange colour wave represents the received light. It should be noted that both the waves are shown with equal amplitude for convenience of understanding. In reality, the amplitude of the reflected wave is much lesser than that of the transmitted wave. It should also be noted that there is an ambiguity in measurement due to the fact that the phase repeats itself after 2π radians. Hence this kind of measurement works without ambiguity only for distances less than half the wavelength corresponding to the modulation

frequency. This will be looked again more deeply in the next chapter in the design of the LIDAR.

1.2 Comparison of the two methods

The following text gives a summary of the advantages and limitations of TOF type Laser Range finder and Phase difference type Laser Range finder.

TOF type LIDAR:

- Measures long range
- Poorer resolution
- High speed electronics required
- No ambiguity in measurement

Phase difference type LIDAR:

- Measures short range
- Better resolution
- Moderately high speed electronics required
- Ambiguity in measurement due to repetition of phase

1.3 Overview of thesis

The rest of the thesis is organized as follows:

Chapter 2 starts with the design specifications, goes into the design of each subsystem and the ground work required for the same.

Chapter 3 deals with the implementation of the circuit, software and mechanical structure.

Chapter 4 shows the results of the work and different tests performed on the LIDAR.

Chapter 5 shows the conclusions and future work on this project

CHAPTER 2
Design and Ground Work

2.1 Design specifications:

As mentioned earlier, the main motivation for this LIDAR is application in Robotics. As the mobile robots navigate mainly indoors, the maximum range required for the LIDAR is limited. Also, as these robots may move in cluttered spaces indoors, they need good resolution in ranging the obstacle. Good resolution also enables the LIDAR to be used in positioning applications. The specifications for the LIDAR have been chosen with these goals in mind. A commercially available Scanning Laser Range finder Hokuyo URG-04LX has been taken as a standard and the specifications of the same were tried to be achieved. The specifications of URG-04LX are as follows:

Range **:** 20mm – 4000mm

Resolution **:** 1mm

Accuracy **:** 10mm or 1% of the distance whichever is higher

Sampling rate **:** 10k samples per second

These specifications were adopted for the LIDAR being constructed too as they are ideally suited for robot applications. It is to be observed that, URG-04LX is capable of scanning the environment around it which is not incorporated in the present design of my LIDAR and this is to be considered a significant difference. This project aims to first make the core LIDAR part which has specifications on par with URG-04LX and then implement the scanning part to it.

2.2 Outline of the system

This chapter deals with the design of the LIDAR. It deals with the considerations and requirements of each of the subsystem. Also, due to usage of non-standard components, the operation of the components at the working frequency had to be checked. As

mentioned in the earlier chapter, the LASER light is modulated at a particular frequency and the phase difference between the transmitted light and the reflected light is measured. This phase difference is proportional to the distance. The block diagram of the LIDAR is shown in Fig. 2.1

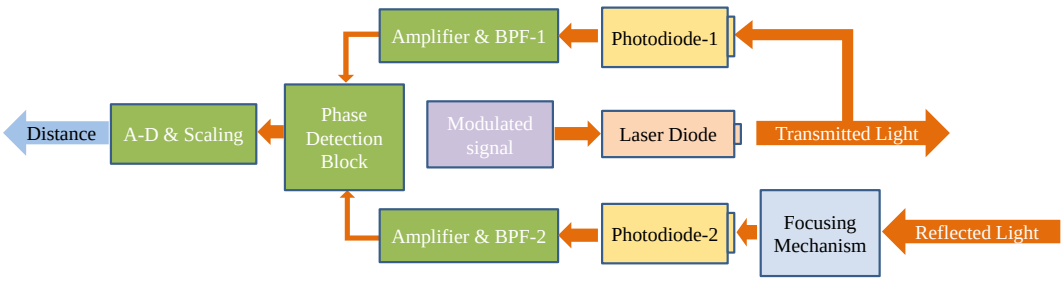

Fig. 2.1: Block diagram of the LIDAR.

As can be seen from the above figure, a modulated signal is given to the Laser diode. Thus the intensity of the Laser diode is increased and decreased at the modulation frequency. A part of this transmitted light is diverted on the Photodiode-1. The light reflected from the target is focussed and then incident on the Photodiode-2. As both of these signals are weak and noisy, Amplifier / BPF stages are required. This amplified signal is given to the Phase detector block which gives an Analog output proportional to the distance. It is converted into digital form and displayed. In the following subsections, calculation of the important parameters like the modulation frequency, Amplifier gain required is shown. In addition to the requirements on modulation frequency and Amplifier gain, the self imposed constraint to use cheap and readily available components added more constraints to the design. This self imposed constraint was adopted mainly to reduce the cost of the LIDAR. With these constraints taken into consideration, different stages of the LIDAR were designed. The design/ground work required for each of the following modules has been explained in detail.

- Modulated Laser transmitter

- Focusing mechanism & diverting mechanism
- Receiver circuit
    - Photodiode circuit
    - Amplifier & Band pass filter circuit
    - Printed Circuit Board (PCB) design
- Phase detector block
- Distance decoding circuit
- PC Interface circuit & software

2.3 Calculation of important parameters

2.3.1 Modulation frequency

The maximum distance that the LIDAR can measure without ambiguity happens when the phase difference between the transmitted and the received light is 2π radians. The desired range for the LIDAR being designed is 4m as mentioned earlier. This means, the phase difference between the transmitted light and received light should be 2π radians when the distance to the target is 4m. The path difference between the transmitted light and the received light in this limiting case is $2x4m = 8m$. Hence, for the modulated wave, $8\,meter$ should correspond to a phase of 2π radians. Or in short, $8\,meter$ is the wavelength of the modulated wave. Hence the modulation frequency is given by

$$\nu = \frac{c}{\lambda} = \frac{c}{2d} = \frac{3 \times 10^8}{2 \times 4} = 37.5\ MHz,$$

where d is the maximum range desired. In this case, $d = 4m$

Fig. 2.2 shows the time frozen image of the intensity of the transmitted and reflected light when the target is at maximum distance $(4m)$. It is to be observed that, the amplitude of the intensity of both the transmitted and reflected light are shown equal, only for convenience in comparing their phases. In reality, the amplitude of the received wave is much smaller than the amplitude of the transmitted wave. Also, the phase difference between the transmitted and reflected wave is 2π radians.

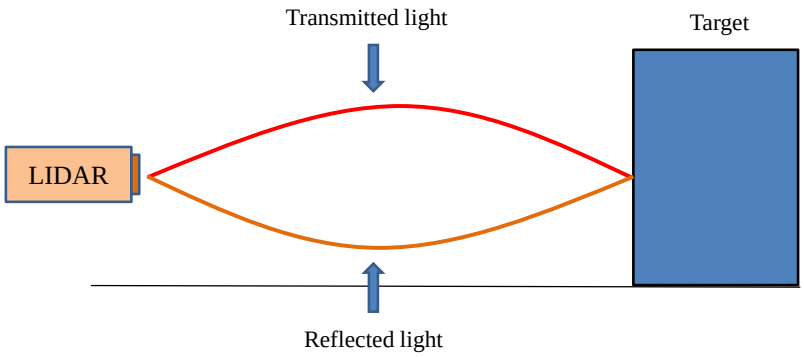

Fig. 2.2: Transmitted and reflected light intensity at different points for maximum range.

2.3.2 Received light power

Only a small part of the light sent out onto the target gets reflected onto the receiver Photodiode. Hence, the reflected light needs to be concentrated onto the photodiode. Thus the power from a larger area is focused onto the photodiode to increase the photocurrent caused. A reasonably large aperture convex lens was used to focus the reflected light onto the Photodiode. The diameter of the convex lens was 75mm.

The power output from the Laser diode is modulated between, about 7mW to 23mW. Thus the amplitude of the power output is 8mW. The light falling on the target is almost same as the light transmitted from the Laser diode.

The reflectivity of white paper is about 0.5. Thus the amplitude of the light power reflected back from the target is about 4mW. As the target surface is a diffused reflective surface, the light is reflected in all directions. The intensity of light reflected by the target in any particular direction is given by

$$\frac{P}{2\pi r^2} cos\theta,$$

where, P is the power reflected from the white screen, r is the distance between the lens and the target and θ is the angle that the line joining the lens and target makes with the normal of the target. For now, let the distance r be 1m.

This light falls on the lens of area = πR^2 where R is the radius of the aperture of the lens. Assuming that the lenses are loss less and that all light focussed by the lens falls on the active region of the Photodiode, the power falling on the Photodiode is given by,

$$\frac{P}{2\pi r^2} cos\theta \times \pi R^2$$

This comes to

$$\frac{4mW}{2 \times \pi \times 1^2} \cos(0) \times \pi \times 0.0375^2 = 2.8\mu W$$

The sensitivity of the photodiode is about 0.5A/W and hence, the photocurrent caused due to the signal in the photodiode is about $1.4\mu A$. As it can be seen, this photocurrent is a very small current and it needs to be converted to a voltage and amplified sufficiently.

2.3.3 Amplification required

Due to some limitations explained in the section 2.4.4.2, the maximum voltage possible from the photodiode is less than 2 mV. An output of 2V is desirable at the output of the amplifier. This requires the gain of the amplifier stage to be 60dB. The input impedance of the amplifier should be very high as compared to the output impedance of the Photodiode circuit. Also, the amplifier should have a Band pass filter built in so that the SNR at the output is sufficiently high.

2.3.4 Signal to Noise Ratio required

As the signal is only at 37.5MHz, it is needless to accumulate noise in all other frequency bands. Hence, the Signal to Noise Ratio (SNR) can be greatly improved by band pass filtering the signal with the centre frequency at 37.5MHz. It is very convenient to combine the amplifier and the Band Pass Filter and should be preferred as it reduces the number of components. In this subsection, the minimum SNR required for effective measurement of phase is derived. The amplifier should attain the aforementioned 60dB gain with the SNR specified.

Firstly, it is assumed that the magnitude of noise variance should be sufficiently smaller than the magnitude of the signal for effective measurement of phase difference. Secondly, the signal received by Photodiode-1 (refer to Fig. 2.1) is much larger than the signal received by Photodiode-2. Hence, only the SNR of Amplifier-2 needs to be considered for calculating the noise in the phase difference. The phase difference measurement block measures the phase difference by checking the difference between zero crossing instants of the two signals. Let the signal magnitude be 1V for convenience. An SNR of 40dB means the standard deviation of the noise is 0.01V. As the slope of a sine wave at zero crossing is 1, this noise in the voltage corresponds to a phase noise of

$$0.01 \times \frac{\pi}{2} = 0.0157\ radians = 0.9°$$

This phase noise corresponds to a noise in measured distance whose variance is

$$\frac{0.9°}{360°} \times 4m = 1cm$$

This noise is acceptable according to our specifications mentioned in section 2.1 and hence an SNR requirement of 40dB was crystallized. The actual noise standard deviation is better than 1cm as the Phase detector in itself has a Low pass filter.

2.4 Design of each module

Now each of the sub sections present the design and ground work require for each of the modules

2.4.1 Modulated Laser transmitter

As one of the main aims of the project was to make the LIDAR in low cost, non standard but easily available components were used. A Laser diode typically used for Laser pointer was intended to be used. These types of Laser diodes do not need any driver circuit but just need a series resistor. This made the design of the transmitter relatively easy. The main problem in designing the transmitter was the question of whether the Laser diode can be modulated at the required frequency i.e. 37.5MHz. Hence a lot of ground work needed to be done to find out that the Laser can actually be modulated at

37.5MHz without any attenuation due to parasitic capacitance or any other internal phenomena. To test if the Laser was getting effectively modulated at 37.5MHz frequency, a Transimpedance amplifier of bandwidth greater than 37.5MHz was used. The circuit diagram of the Transimpedance amplifier is shown in Fig. 2.3

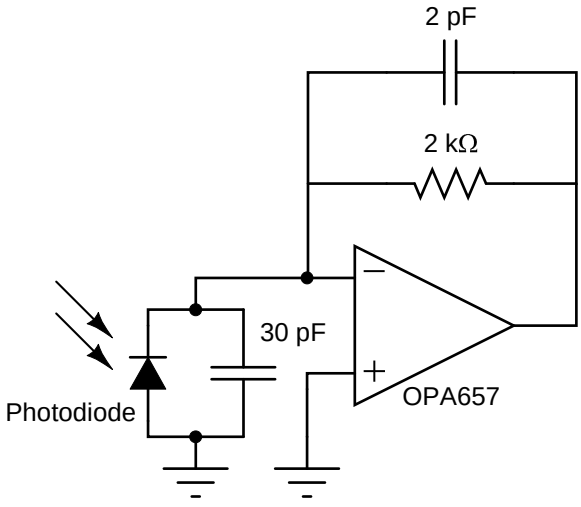

Fig. 2.3: Transimpedance amplifier to test the Laser diode.

OPA657 being a non unity gain stable amplifier, care needs to be taken that the Opamp does not go into instability. This is achieved by putting a suitably high resistor as transimpedance and choosing the capacitor values such that

$$\frac{C_f}{C_t + C_f} \leq \frac{1}{Minimum\ gain\ possible} = \frac{1}{7}$$

where, C_f is the capacitance in feedback and C_t is the capacitance in parallel to the photodiode. Also, the photodiode has a parasitic capacitance parallel to it. This parasitic capacitance is for the photodiode used is about 10pF.

Fig. 2.4 shows the simulated magnitude response of the Transimpedance amplifier. The input from the photodiode is simulated by a current source with a DC current of $30\mu A$ and an AC current of $20\mu A$. The simulation was performed in LTSpice simulator. The simulation clearly shows a bandwidth greater than 37.5MHz and hence can in principle be used to test the modulation of the Laser diode. This transimpedance amplifier was

implemented on a PCB and the Laser diode + transimpedance amplifier was tested. The total system showed a bandwidth of about 50MHz which is more than 37.5 MHz.

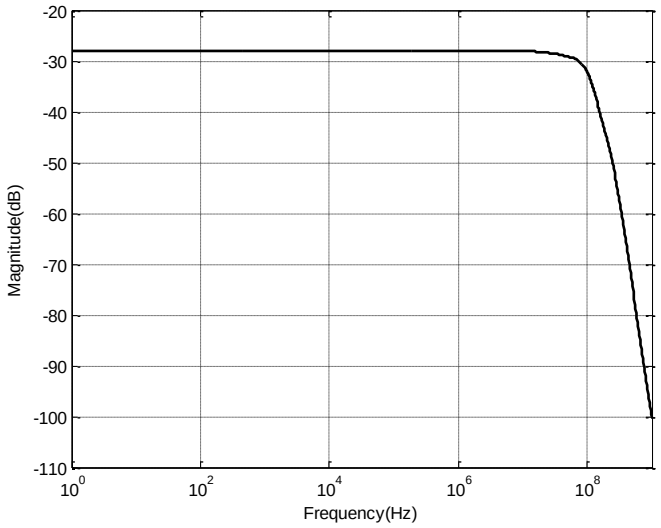

Fig. 2.4: Magnitude response of the Transimpedance amplifier.

Hence it can be concluded that the Laser diode is getting modulated effectively even at 37.5MHz.

2.4.2 Focusing Mechanism & Diverting Mechanism

2.4.2.1 Focusing Mechanism

As mentioned already, the intensity of light reflected from the target is very low. For enough amount of light to fall on the photodiode, it needs to be focused. Convex lens of sufficiently big aperture needs to be used for this purpose. The lens assembly should be placed such that the focus of the effective lens falls precisely on the photodiode, i.e. the separation between the lens and the photodiode should be equal to the focal length of the lens. Due to an upper limit on the board size, this separation between the lens and the photodiode can be a maximum of 100mm. Hence, the focal length of the lens should be less than 10cm. To meet the requirements of low focal length and high aperture diameter without aberration, multiple lenses need to be used. The focusing mechanism for this

LIDAR is designed with 3 convex lenses each of focal length of 225mm and aperture diameter of 75mm. Fig. 2.5 illustrates the placement of the lenses.

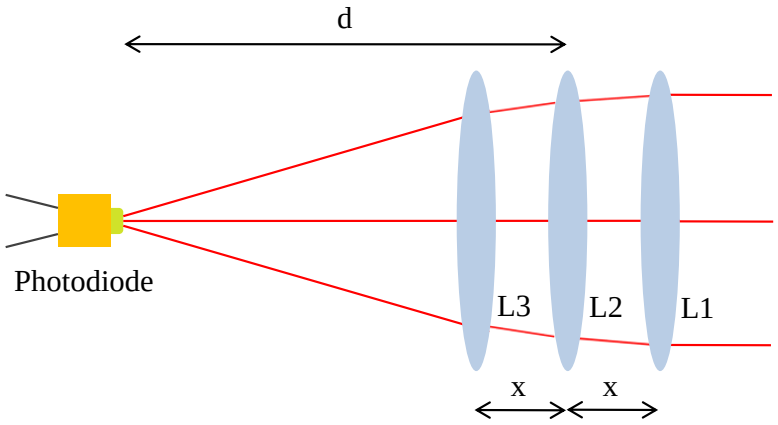

Fig. 2.5: Lens mechanism.

The following derivation shows the placement of each of the three lenses so that the distance between the effective lens and the photodiode is equal to the effective focal length.

Effective focal length (f_{eq}) of two convex lenses placed at a separation x is given by

$$\frac{1}{f_{eq}} = \frac{1}{f_1} + \frac{1}{f_2} - \frac{x}{f_1 f_2}$$

where, f_1 and f_2 are the focal lengths of each of the lenses. For two convex lenses, the equivalent lens lies in between both the lenses at a distance, $f_{eq}\, x / f_2$ from the lens whose focal length is f_1

Consider, f to be the focal length of each of the lens. From Fig. 2.5, the separation between adjacent lenses is x and the separation between L2 and the photodiode is d. Then the effective focal length of the lenses L1 and L2 put together is given by the expression,

$$\frac{1}{f_{12}} = \frac{1}{f} + \frac{1}{f} - \frac{x}{f^2} = \frac{2f - x}{f^2}$$

This effective lens can be considered to be placed at a position

$$\frac{f_{12}x}{f_1}$$

to the right of L2. Hence, the separation between, L3 and equivalent lens of L1 & L2 is

$$x_{12-3} = x + \frac{f_{12}x}{f_1} = \frac{3fx - x^2}{2f - x} = \frac{x(3f - x)}{2f - x}$$

The effective focal length of all the three lenses put together is given by

$$\frac{1}{f_{123}} = \frac{1}{f} + \frac{1}{f_{12}} - \frac{x_{12-3}}{ff_{12}}$$

$$= \frac{1}{f} + \frac{2f - x}{f^2} - \frac{3f - x}{f^3}$$

Hence, f_{123} is given as

$$f_{123} = \frac{f^3}{3f^2 - 4fx + x^2} = \frac{f^3}{(3f - x)(f - x)}$$

The separation between the effective lens and L3 is given as

$$x_{3-123} = \frac{f_{123}x_{12-3}}{f} = \frac{f^3}{(3f - x)(f - x)} \frac{x(3f - x)}{2f - x} \frac{1}{f}$$

$$= \frac{f^2 x}{(f - x)(2f - x)}$$

Hence, the distance of the effective lens from the photodiode is

$$x_{pd-123} = d - x + x_{3-123}$$

$$= d - x + \frac{f^2 x}{(f - x)(2f - x)}$$

$$= d - x\left(\frac{f^2 + 3fx + x^2}{(f - x)(2f - x)}\right)$$

For the lens mechanism to focus properly on the photodiode, the effective focal length should be equal to the separation between the photodiode and the effective lens. This yields the following equation.

$$f_{123} = x_{pd-123}$$

$$i.e. \quad \frac{f^3}{(3f - x)(f - x)} = d - x\left(\frac{f^2 + 3fx + x^2}{(f - x)(2f - x)}\right)$$

The above equation cannot be solved independently for x and d. x = 20mm seems a suitable value for the separation between the lenses. This value of x is plugged into the equation and d is calculated. The value of d is calculated to be 99mm. Hence, the middle lens should be place at a distance of 99mm from the photodiode.

2.4.2.2 Diverting Mechanism

A part of the transmitted wave needs to be diverted onto the Photodiode-2 (Refer to Fig. 2.1) This light wave serves as the reference copy of the phase and the received light is compared with this to obtain the phase difference. The optics to divert the light consists of a partially reflecting mirror kept at an angle of 45° to the direction of light. The diverted beam is again diverted by the use of a fully reflecting mirror placed at an angle of 45° to the partially reflected beam. This double deflected beam should be such that it falls on Photodiode-2. Fig. 2.6 shows the designed mechanism to achieve the same.

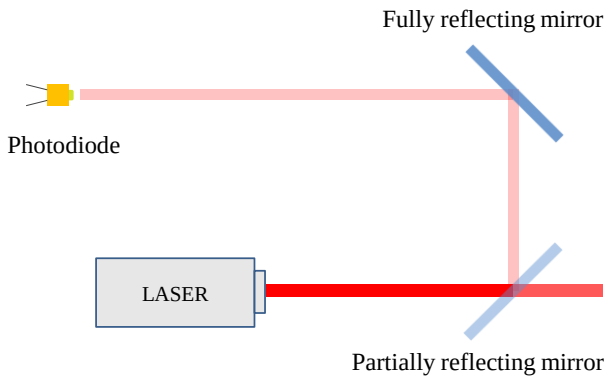

Fig. 2.6: Beam diverting mechanism for reference light wave.

2.4.3 Photo-detector circuit

The Photo-detector circuit is the front end of the receiver circuit. When light falls on the photodiode, a voltage signal should be seen at the output of the Photo-detector circuit. Though the Photo-detector circuit is followed by an amplifier cum band pass filter circuit, it is very desirable to have band pass filtering in this stage itself. One of the main advantages of having band pass action in the Photo-detector stage itself is that the Photo-current caused due to stray DC light is filtered and thus output saturation does not happen. The output impedance of this stage must be low as it may be followed by a low input impedance amplifier. Three main designs have been considered for Photo-detector circuit. They are

- Current sensor + Unity gain buffer
- Transimpedance amplifier
- Band pass Transimpedance amplifier

The design, analysis, pros and cons of each design are presented in the following sub sections.

2.4.3.1 Current sensor + Unity gain buffer

As the name suggests, the current from the photodiode is pushed into an R, L & C kept in parallel. The L & C are chosen such that they resonate at the operating frequency i.e. 37.5MHz. The voltage at the junction of the photodiode and the RLC network is sensed and followed by a Unity gain buffer made out of OPA656 Opamp. For the LC network to resonate at 37.5 MHz, L and C should be chosen such that

$$\frac{1}{2\pi\sqrt{LC}} = 37.5MHz$$

Choosing Inductor values greater than 1μH requires the capacitor value to be few tens of pico-farads. This causes the PCB parasitic capacitances to affect the resonance frequency. Hence, a low inductance value needs to be chosen. Due to easy availability of 120nH inductors, they were chosen for the design. Inductance of 120nH corresponds to a capacitance of 150pF. The photodiode has its own parasitic shunt capacitance of about

10pF. Hence, a capacitance of 140pF was kept in parallel to the inductor. It should be noted that the capacitance at the input of the Opamp is very less and thus has been neglected. Fig. 2.7 shows the circuit diagram for the Current sensor + Unity gain buffer type photo-detector circuit.

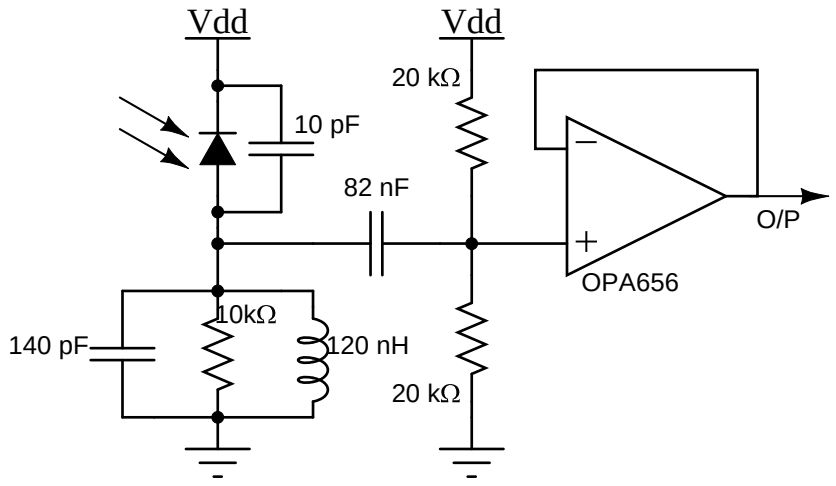

Fig. 2.7: Current sensor + Unity gain buffer type photo-detector circuit.

AC analysis of the above circuit has been performed in LTSpice to find out the gain at resonant frequency. As found out in section 2.3.2, a white target placed at a distance of 1m, ideally, causes an AC current of 1.4μA riding over a DC offset of 2.8μA. This current is considered standard for comparing all the three designs of the photo-detector circuits. The Photodetector is simulated by an AC current source of amplitude 1.4μA riding over a DC current offset of 2.8μA. Noise analysis was performed on the photo-detector circuit assuming that photodiode is the noiseless source. Noise analysis gives a Noise Spectral Density (NSD) plot. The NSD when squared and integrated from 1Hz to 1THz gives the variance of the noise. Another parameter that should be seen while comparing the different photo-detector circuits is the slope of the phase response at resonant frequency. As the primary measurement is based on phase difference, we want the phase induced by the circuit to be equal for both Photodetector-1 and Photodetecto-2. If the phase response of the photo-detector circuit is very steep at the resonant frequency, small mismatches in the L & C component values cause large and unwanted circuit induced phase difference between the two paths. Though steep phase response is

inevitable at the resonant frequency, the steepness should be made as minimum as possible.

Fig. 2.8 shows the magnitude response of the photo-detector circuit. It can be seen that the output voltage at the resonant frequency is about -56dB and the resonant frequency is 37.4MHz.

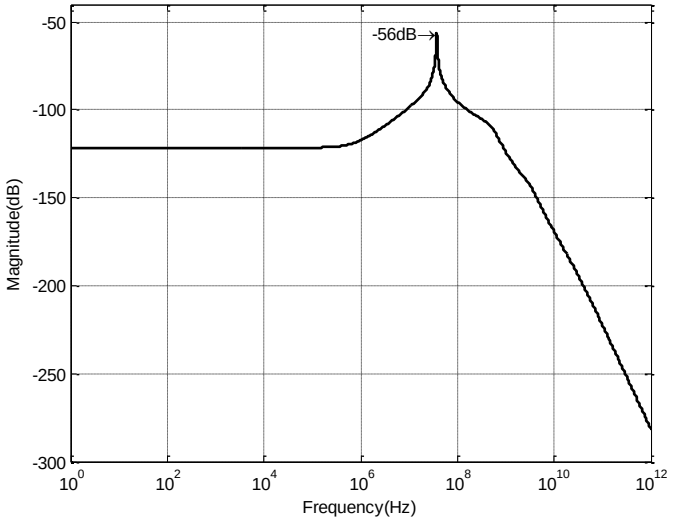

Fig. 2.8: Magnitude response of Current sensor + Unity gain buffer circuit.

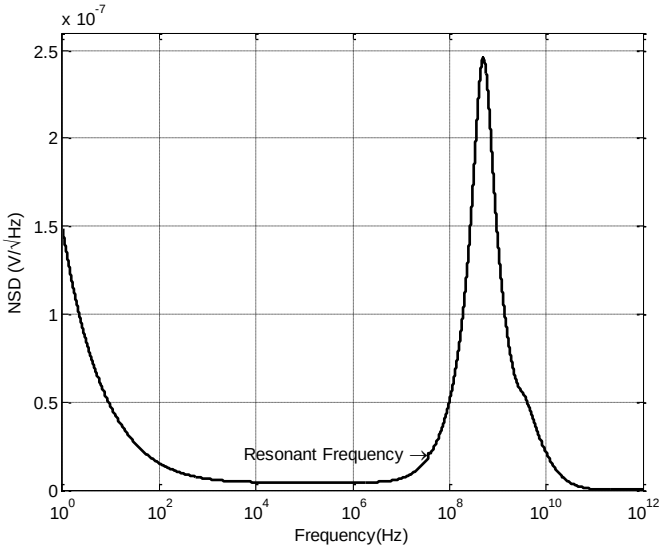

Fig. 2.9: Noise Spectral Density of the Current sensor + Unity gain buffer circuit.

Fig. 2.9 shows the NSD of the Photodetector circuit being discussed. When integrated over all effective frequencies, the noise variance comes out to be -42dB. Though this looks extraordinarily large as compared to the signal, filtering in the following stages makes the SNR much better. Also, the rate of slope of the phase response at the resonance frequency is $-0.11°$ /kHz. Another important parameter to note is the magnitude of NSD at the signal frequency. From the above diagram it can be seen that the magnitude of NSD at 37.4MHz is $20nV/\sqrt{Hz}$.

2.4.3.2 Transimpedance amplifier

Transimpedance amplifier consists of an Opamp with a resistor in feedback. Any input current passes through the resistor and results as a voltage at the output of the Opamp. Fig. 2.10 shows the circuit diagram of the Transimpedance amplifier.

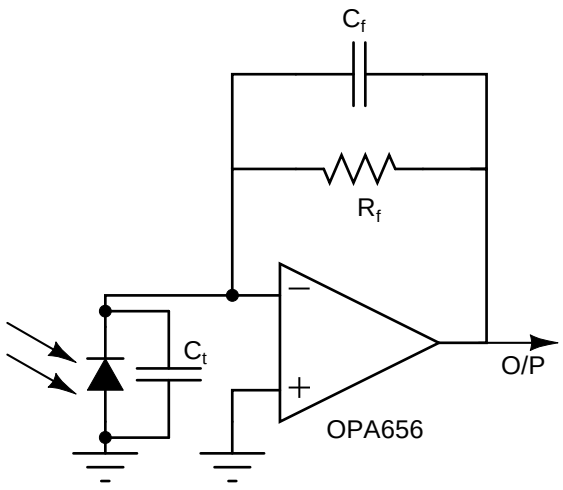

Fig. 2.10: Transimpedance amplifier circuit diagram.

As the input impedance of the Opamp is very high compared to the feedback resistance (R_f) most of the photocurrent flows into the feedback resistor. This feedback resistor is known as Transimpedance. There is a capacitor (C_f) kept in parallel to the feedback resistance. One particular value of this capacitor maximises the bandwidth of the Transimpedance amplifier. This value of C_f which maximises the bandwidth of the amplifier is given by

$$C_f = \sqrt{\left(\frac{2\omega_u R_f C_t - 1}{\omega_u^2 R_f^2}\right)}$$

where, C_t is the parasitic capacitance parallel to the diode and ω_u is the unity gain frequency of the Opamp. In the above circuit, ω_u is 1257×10^6 rad/s and C_t is 10pF. For different values of R_f ranging from 500Ω to 3kΩ, the feedback capacitance is calculated. The output voltage magnitude (in dB) of the transimpedance amplifier at 37.5MHz is noted for each case. These values are tabulated in Table 2.1.

R_f	C_f	**Output voltage (in dB)**
0.5kΩ	5.4pF	-40dB
1kΩ	3.9pF	-35dB
1.5kΩ	3.2pF	-32dB
2kΩ	2.8pF	-30dB
2.5kΩ	2.5pF	-30dB
3kΩ	2.3pF	-29dB

Table 2.1: Output voltages for different Transimpedances.

From the above values 2kΩ was chosen to be the transimpedance. Fig. 2.11 gives the circuit diagram with the values.

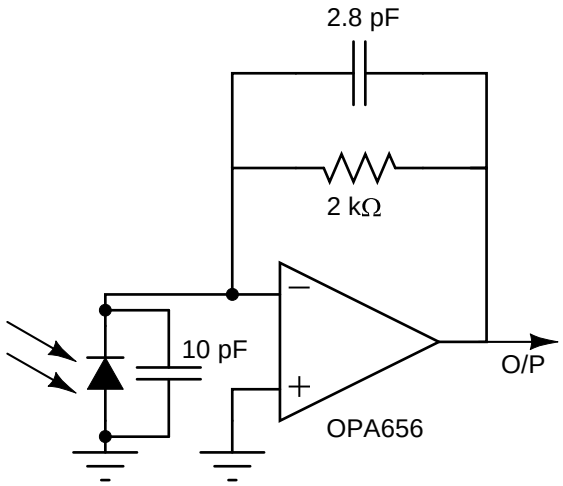

Fig. 2.11: Transimpedance amplifier with component values shown.

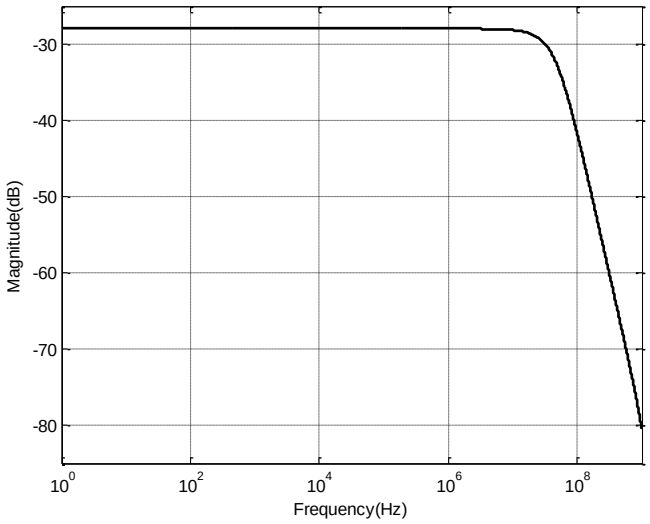

Fig. 2.12: Magnitude response of the designed Transimpedance amplifier.

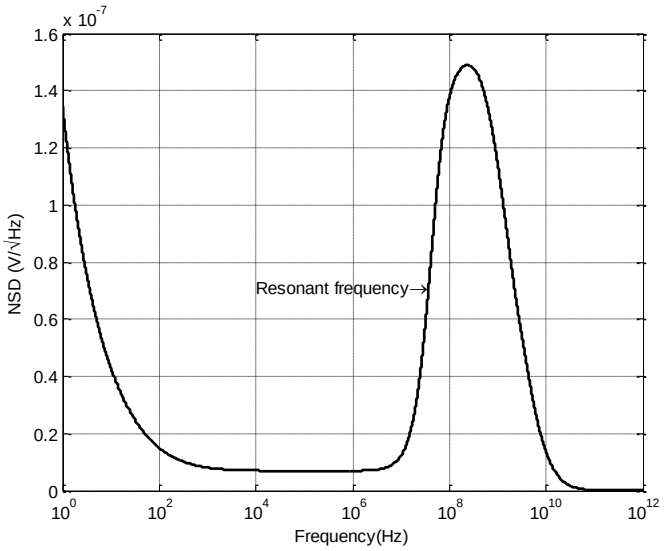

Fig. 2.13 Noise Spectral Density of the Transimpedance amplifier designed.

Fig. 2.12 shows the magnitude response of the designed Transimpedance amplifier. Fig. 2.13 shows the Noise Spectral density of the Transimpedance amplifier. The NSD has been integrated over 1Hz to 1THz frequencies to give the noise variance. This noise variance was computed to be -44dB. Also, in this Photodetector circuit, there is no band pass filtering action. This may lead to accumulation of lot of noise caused due to the photodiode. Also, the DC component of light remains unfiltered and there is a possibility

of saturation. The slope of the phase response at the resonance frequency is $-2.5°$/MHz. From the above NSD plot, the magnitude of NSD at the signal frequency i.e. 37.4 MHz is $72nV/\sqrt{Hz}$.

2.4.3.3 Band pass Transimpedance amplifier

As the Transimpedance amplifier accumulates noise from DC, and might saturate the output, a variant of Transimpedance amplifier was thought. Along with the feedback resistor, a feedback inductor and capacitor are placed. The L & C values are chosen such that they resonate at 37.5MHz. Though this looks to be a good option, the stability of the resulting circuit was not positive. Fig. 2.14 shows the circuit diagram of the proposed circuit. OPA656 was used for the Opamp. L, C & R values were chosen to be 120nH, 150pF and 10kΩ respectively for the same reasons mentioned in section 2.4.3.1. Fig. 2.15 shows the frequency response of the loop gain zoomed around the problematic area. On close observation of the loop gain, it can be seen that at the place where the magnitude becomes unity, the phase becomes as low as 240^0 which clearly results in instability.

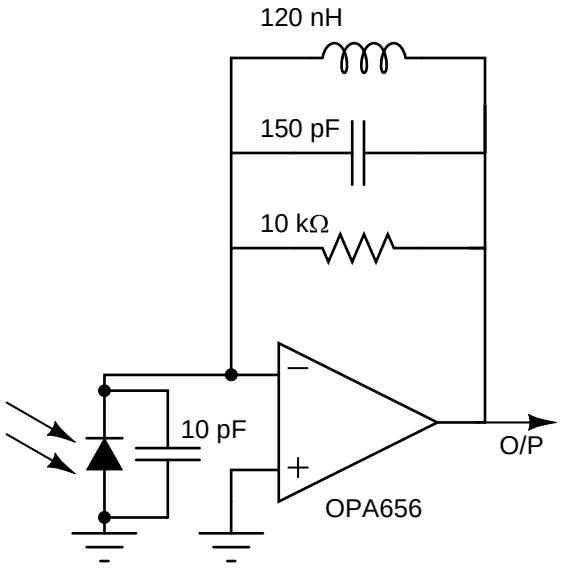

Fig. 2.14: Band pass Transimpedance amplifier.

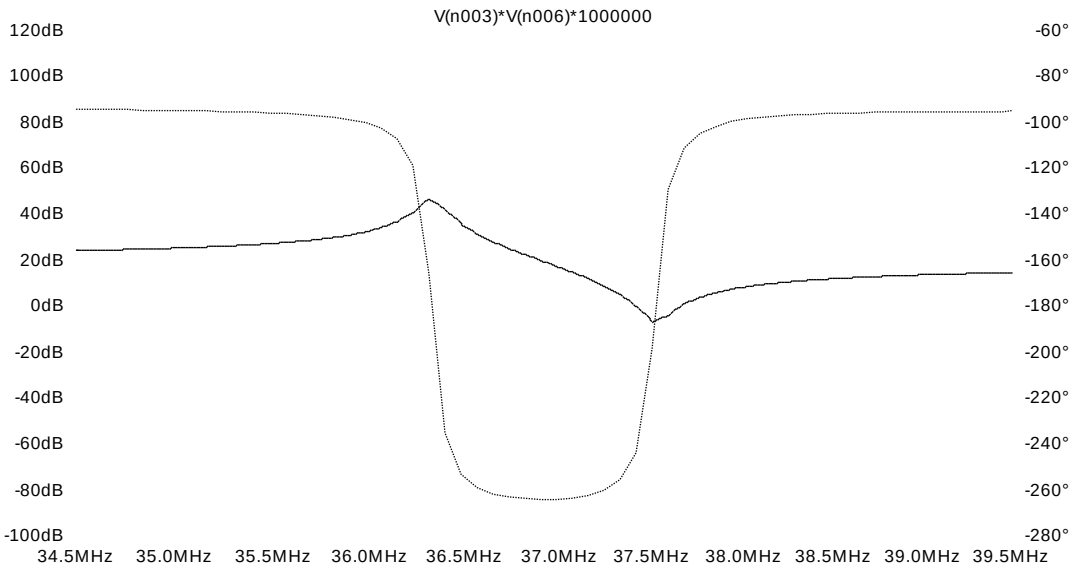

Fig. 2.15: Frequency response of the loop gain of Band pass Transimpedance amplifier.

2.4.3.4 Comparison between the three Photodetector circuits

In this section a comparison between the three photodiode circuits is made and the best one is selected. The characteristics of each of the circuits are as follows.

Current sensor + Unity gain buffer:

- Output voltage = -56dB.
- Noise variance = -42dB.
+ NSD magnitude at 37.5MHz = $20nV/\sqrt{Hz}$.
+ NSD peak more separated from the signal frequency.
+ Filters optical noise and DC noise.
- Slope of phase response at 37.4MHz = $-0.11°/kHz$

Transimpedance amplifier:

+ Output voltage = -30dB (31mV).
+ Noise variance = -44dB (SD of 6.3mV).
- NSD magnitude at 37.5MHz = $72nV/\sqrt{Hz}$.
- NSD peak closer to the signal frequency.
- Does not filter optical noise or DC noise and hence subject to risk of saturation

+ Slope of phase response at 37.5MHz = $-2.5°/MHz$
- Very low capacitance needed for C_f is difficult to achieve accurately and the gain is highly dependent on C_f

Band pass Transimpedance amplifier:

- Risk of instability

From the above summary, the pros of Current sensor + Unity gain buffer design were considered more important than the pros of Transimpedance amplifier, due to which Current sensor + Unity gain amplifier was selected for the final circuit.

2.4.4 Amplifier & Band pass filter circuit

As seen earlier, the SNR of the output signal from the photo-detector circuit is very low. Hence filtering of the signal is required. Also, as the magnitude of the signal itself is very low, it needs to be amplified. The amplifier circuit takes care of both these tasks. The main requirement of this amplifier circuit is to make the signal as high as possible and make the SNR as low as possible. Two main designs have been considered for the amplifier circuit. They are

- Opamp based amplifier
- Transistor amplifier with Opamp buffer

Both these designs are considered and compared in the next two subsections.

2.4.4.1 Opamp based amplifier

This design consists of two cascaded negative feedback amplifiers. To achieve high bandwidth, the design was made with OPA847 Wideband Operational Amplifier and simulated in LTSpice. The Gain-Bandwidth product of this Opamp is 3.9GHz for gains above 50. The ratio of the resistances was chosen such that the gain at 37.5MHz was maximised. This ratio of resistances corresponds to a gain of 50 for one stage of the amplifier. Also, to decrease the effect of noise two band-pass filters with resonant

frequency at 37.5MHz were inserted at the output of each Opamp. Fig. 2.16 shows the circuit diagram for the Opamp amplifier being considered.

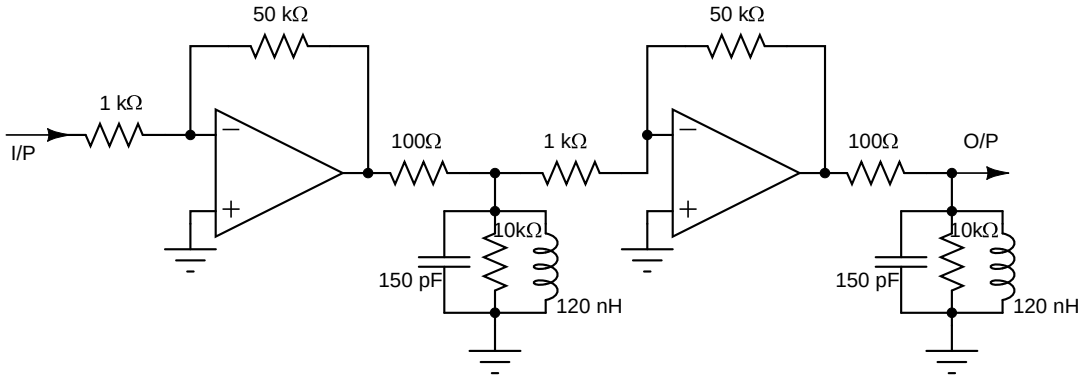

Fig. 2.16: Opamp based amplifier circuit.

The Opamp based amplifier circuit was cascaded next to the photo-detector circuit and tested for a standard AC current input of 1.4μA to the photo-detector (1.4μA is the photo-current produced with white screen target placed at 1m). AC analysis of the above circuit was performed for the above given input to the photo-detector. The circuit show a peak amplitude of 7.5dB (2.3V) at the resonant frequency, 37.4MHz. The magnitude response of the photo-detector & amplifier circuit put together is shown in Fig. 2.17.

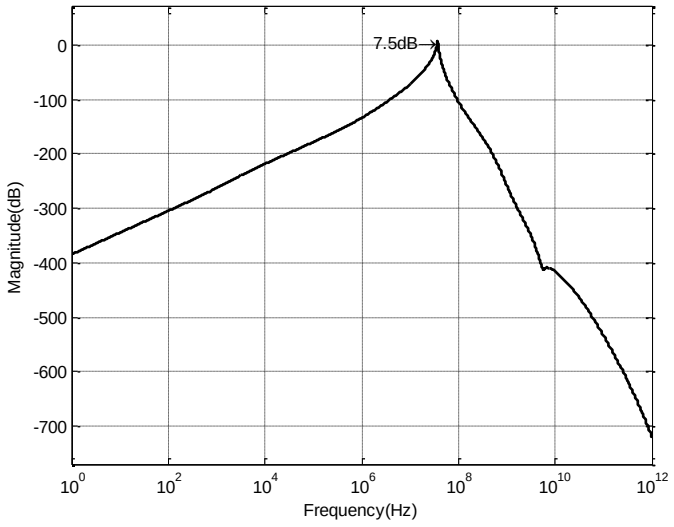

Fig. 2.17: Magnitude response of Opamp based amplifier circuit.

Noise analysis was also performed on the same circuit to get the Noise spectral density graph. The NSD of the Opamp amplifier circuit is shown in Fig. 2.18. The NSD was squared and integrated from 1Hz to 1THz to give the noise variance. The noise variance was calculated to be -21dB. This noise corresponds to a standard deviation of about 90mV. The resulting SNR of the circuit is about 28.5dB.

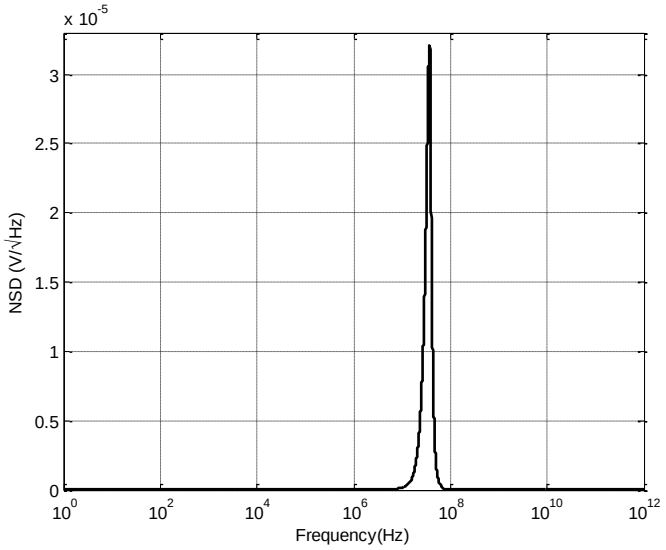

Fig. 2.18: Noise Spectral Density of Opamp based amplifier.

2.4.4.2 Transistor amplifiers with Opamp buffer

This design consists of two LC tuned Common Emitter amplifiers with a buffer circuit in between. Both the amplifiers have been tuned for 37.5 MHz. The buffer circuit is necessary to prevent loading of the first stage due to the second stage. The buffer circuit is made from unity gain configuration of an OPA656 Operational amplifier. 2N918 NPN high frequency transistor has been selected as the transistor for the common emitter amplifier. This selection was done mainly based on its high Transition frequency (f_T) of 900MHz and low junction capacitances. In order to achieve very high gain in least number of stages, the small signal emitter degenerate resistance (R_E) was made zero. The disadvantage of making R_E zero is that the input impedance becomes very low. The L & C filter the noise to make the signal better.

Some of the circuit parameters of each of the common emitter amplifier stage are given below:

- DC Collector current = 3.9mA
- Input impedance = 130Ω (low)
- Output impedance = 1.5kΩ
- Equivalent load resistance = 1.5kΩ
- Transconductance = 156mS
- Expected gain = 47dB
- Simulated gain = 41dB
- Resonant frequency = 37.1MHz
- Quality factor = 49

Equivalent load resistance is the parasitic series resistance of the inductor which looks as a shunt resistance to the L & C at resonant frequency. The circuit diagram of amplifier is shown in Fig. 2.19.

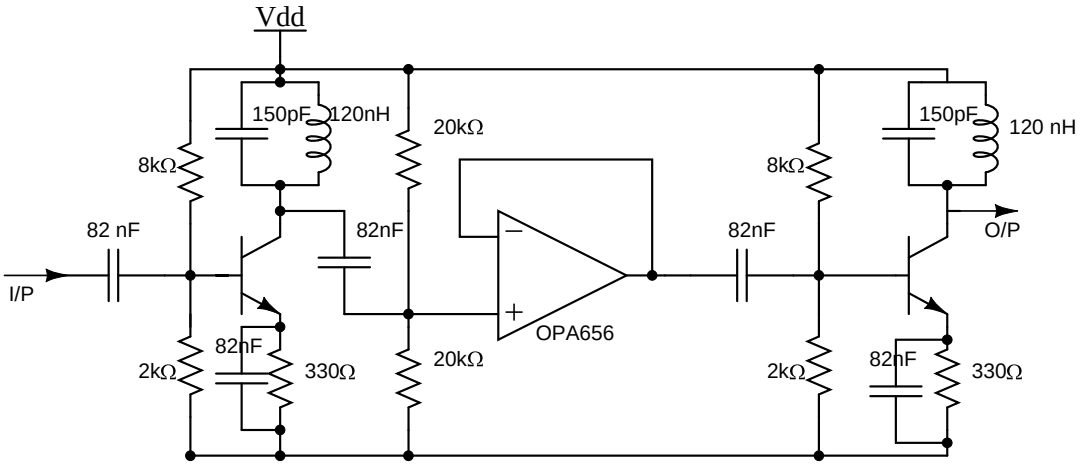

Fig. 2.19: Transistor amplifier with Opamp buffer.

The above amplifier was kept cascade with the photo-detector circuit and simulated in LTSpice. A standard AC current input of 1.4μA was given to the photo-detector. As mentioned earlier, this is the photo-current produced when a white screen target is placed at a distance of 1m. AC analysis was performed on the Photodetector + amplifier circuit. For the given input, a peak output voltage amplitude of 15dB (5.6V) was observed. The magnitude response of the Photodetector + amplifier circuit is shown in Fig. 2.20

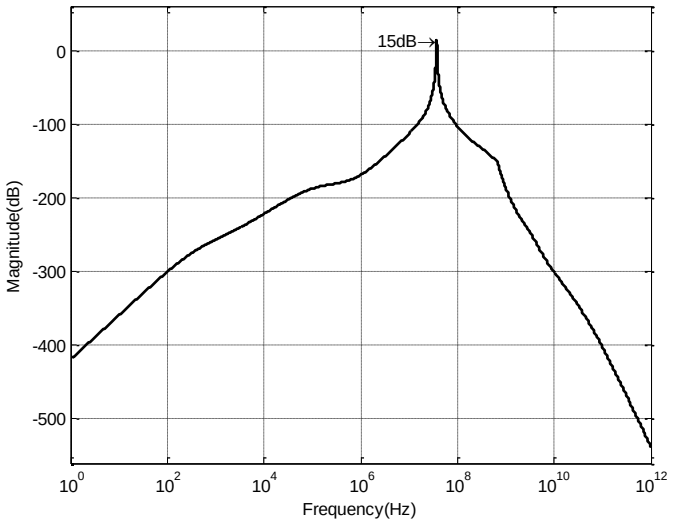

Fig. 2.20: Magnitude response of Photodetector + transistor amplifier.

Noise analysis was performed on the Photodetector + transistor amplifier circuit. The Noise spectral density plot can be seen in Fig. 2.21. This noise was integrated from 1Hz to 1THz to give the noise variance. This noise variance was computed to be -35dB. This corresponds to a noise standard deviation of 18mV. The signal to noise ratio in this case is about 50dB.

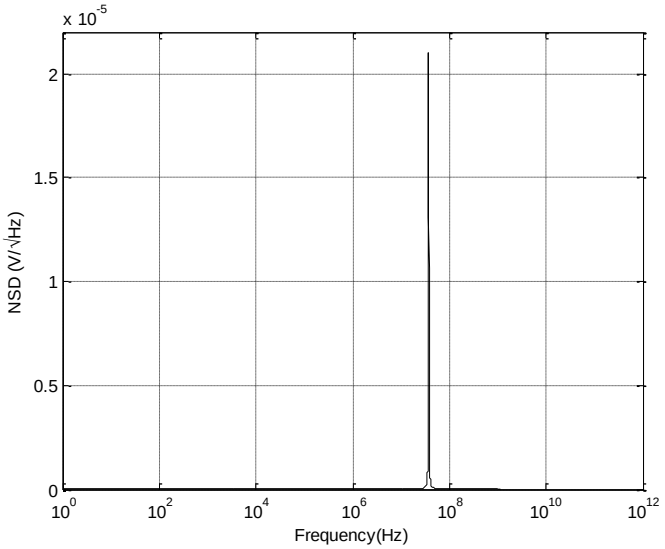

Fig. 2.21: Noise Spectral Density of Photodetector + transistor amplifier with Opamp buffer.

2.4.4.3 Comparison

The characteristics of both the amplifier circuits explained above are summarized below. It is to be observed that both of them have been simulated with the same Photodetector circuit. The same input of 1.4μA has been given in both the cases to maintain uniformity.

Opamp amplifier:

- Output amplitude : 7.5dB (2.3V)
- Noise variance : -21dB (SD of 90mV)
- SNR : 28.5dB
- No. Opamps used : 3

Transistor amplifier with Opamp buffer:

- Output amplitude : 15dB (5.3V)
- Noise variance : -35dB (SD of 18mV)
- SNR : 50dB
- No. Opamps used : 2

From the above values, the choice of the amplifier cum band pass filter circuit is clearly the 'Transistor amplifier with Opamp buffer' circuit.

2.4.5 Phase detector circuit

The phase detector circuit finds out the phase difference between the two signals. An Analog Devices - AD8302 RF/IF phase detector IC is used as the phase detector. The phase detector has two input channels into which the reference and reflected signals can be fed. Inside the phase detector there is a series of amplifiers which amplify the signal to reach rail to rail. There is a mechanism for offset cancellation so that only the AC component of the signal is amplified and not the DC component. The two square wave signals thus produced are multiplied and the output is filtered to give a voltage proportional to the phase difference. Thus the output of the AD8302 IC is a voltage between 0 and 1.8V, varying linearly with the phase difference (proportionality constant

is negative). As mentioned above AD8302 uses a multiplier type of phase detection technique. With this type of technique, it is not possible to distinguish angles above 180^0 from angles below 180^0. Given below are some important specifications and features of the phase detector IC.

Specifications:

- Maximum measurement frequency : 2.7GHz
- Phase scaling factor : 10mV/degree
- Maximum phase measurement bandwidth : 30MHz
- Maximum input voltage amplitude : 0.7mV

Features:

- Provision to reduce maximum bandwidth to any value below 30MHz
- Stable 1.8V reference voltage
- Provision to change the scaling factor

As a bandwidth of 30MHz is not required for our phase difference measurement, external filtering capacitors are kept and the bandwidth is reduced to about 1 MHz. According to the datasheet, these capacitances can be calculated by the formula,

$$C_{AVE}(pF) = \frac{T(ns)}{3.3}$$

where, T is the time over which the results need to be averaged. In the present case, T was chosen to be 1μs so as to allow for a maximum possible Laser range finder's sampling rate of 500 kHz. This averaging time results in a C_{AVE} of about 300pF. Suitably high capacitors can be used for low pass filter required for the offset cancellation mechanism.

Care was taken so that the maximum voltage sensed by the phase detector IC does not exceed 0.7V in amplitude as the maximum voltage that can be given to the IC input is 0.7V. The IC comes in a 14-pin TSSOP package for which the PCB was designed.

2.4.6 PCB design

The design conceptualised in the above sections needs to make use of OPA656, AD8302 both of which are SMD ICs. Also, the speed at which the circuit operates is moderately high speed. Due to both of these reasons, a PCB is required to be made for the circuit. A PCB was designed in EAGLE. A 2-sided board sufficed for the circuit. Fig. 2.22 shows the PCB design.

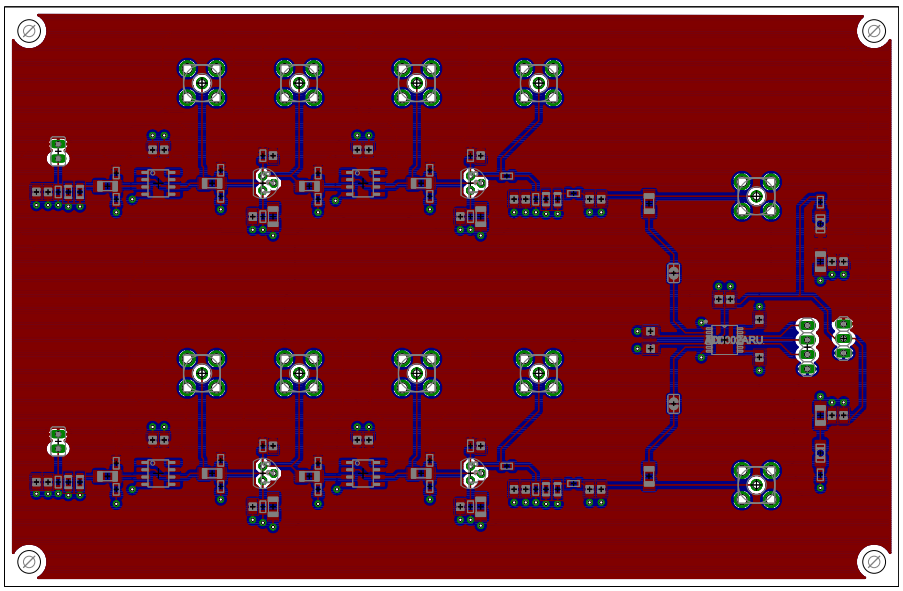

Fig: 2.22 PCB layout (top view).

The following cares have been taken while designing the PCB

- The paths travelled by received signal and the reference signal are the same.
- Both the receiver circuits are exactly identical.
- The components are placed as close as possible (given the constraint that both the photo-diodes should be separated at least by a distance equal to the radius of the aperture of the focusing lens.
- An extra component space is provided for the tuning L & C to provide for placement of extra components if required.

- Provisions for SMA connectors have been provided at multiple places in order to test the circuit easily.
- Provisions for bypass capacitors have been provided at multiple locations.

The figures, Fig. 2.23 & 2.24 show the top & bottom layers of the PCB respectively.

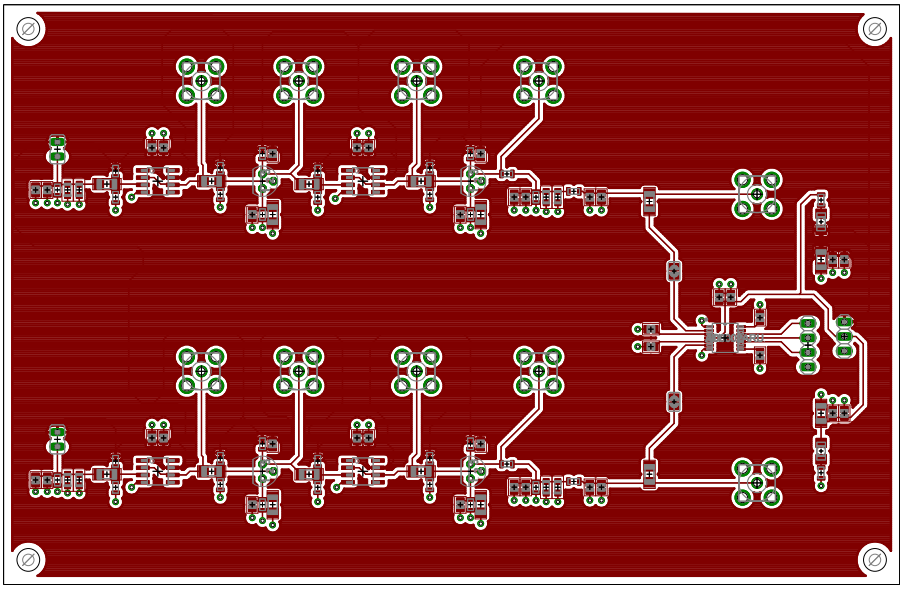

Fig. 2.23: PCB layout (top layer).

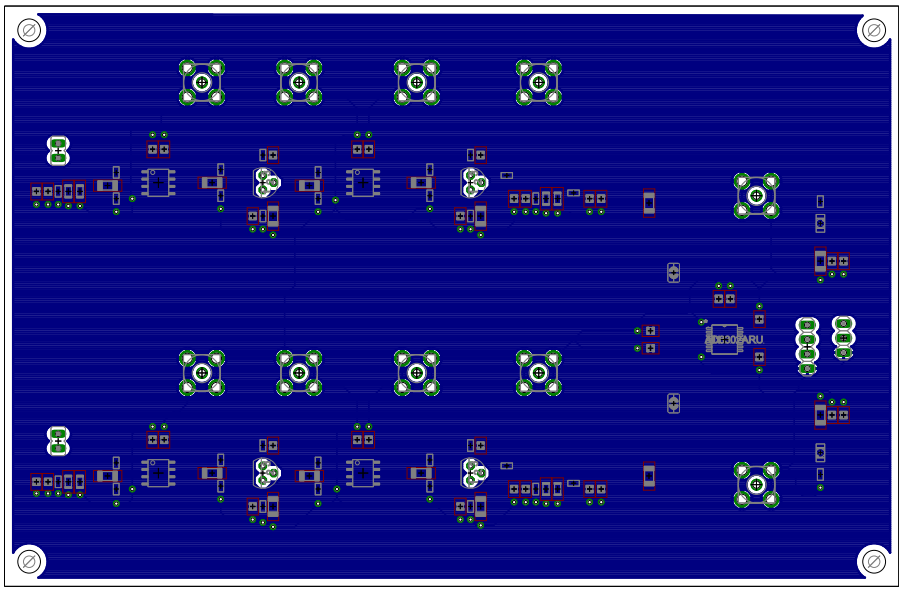

Fig. 2.24: PCB layout (bottom layer).

2.4.7 Distance decoder circuit

As already mentioned, the AD8302 IC gives an analog output which varies as,

$$V_{out} = 1.8 - \phi \times 10mV/^{\circ}$$

where, ϕ is the phase difference in radians. This analog output voltage needs to be converted into a digital code, scaled suitably and the distance needs to be displayed on a seven segment display. All the above functions, i.e. Analog to Digital conversion, scaling and sending appropriate signals to the seven segment display can be performed in an ATMega8 microcontroller. Hence, an ATMega8 microcontroller has been used for the same. The block diagram of the distance decoder circuit is shown in Fig. 2.25.

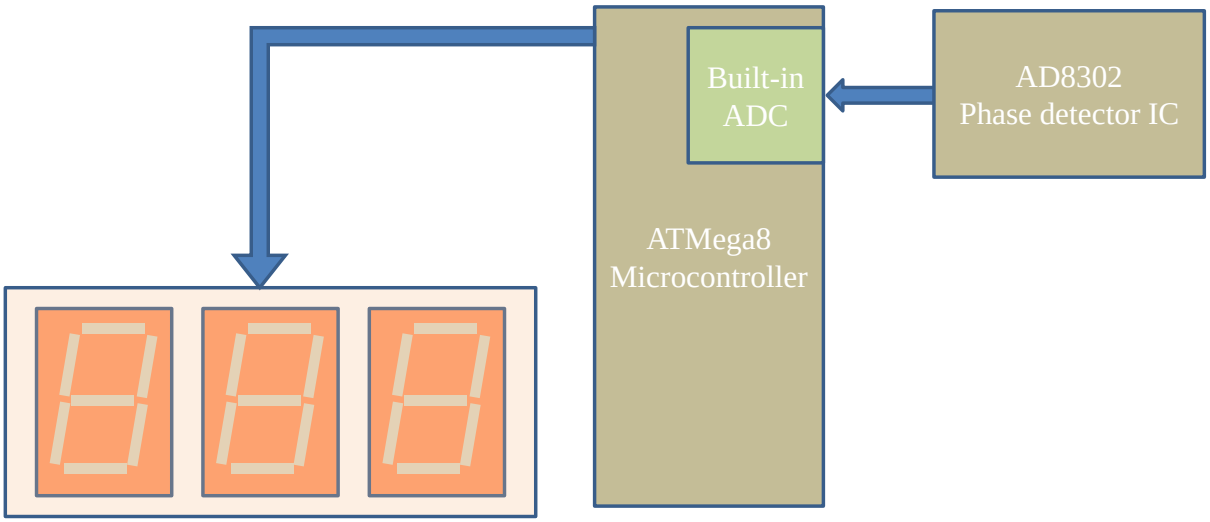

Fig. 2.25: Block diagram of distance decoder circuit.

To perform all the above tasks in a microcontroller, a C language code was written in WinAVR interface. This C code is converted into an assembly file and then burnt into the microcontroller using USBTiny ISP programming interface. The microcontroller samples the output of AD8302 at a rate of 1 kHz and displays it on the seven segment displays at the same refresh rate. The ADC used is a 10-bit successive approximation type ADC. The phase detector circuit detects a maximum phase of 180°. This corresponds to a distance

of 2m. The ADC can digitize the 0-1.8V signal with a resolution of 10-bits. This means that the minimum resolution of distance measurement corresponds to $2m/2^{10}$ = 1.953mm.

2.4.8 PC Interface circuit & software

A microcontroller based serial interface circuit was made to acquire data onto a computer. The main purpose of data acquisition on PC was to analyse large chunks of data and characterize the LIDAR's error in measurement. The block diagram of the PC interface circuit is given in Fig. 2.26.

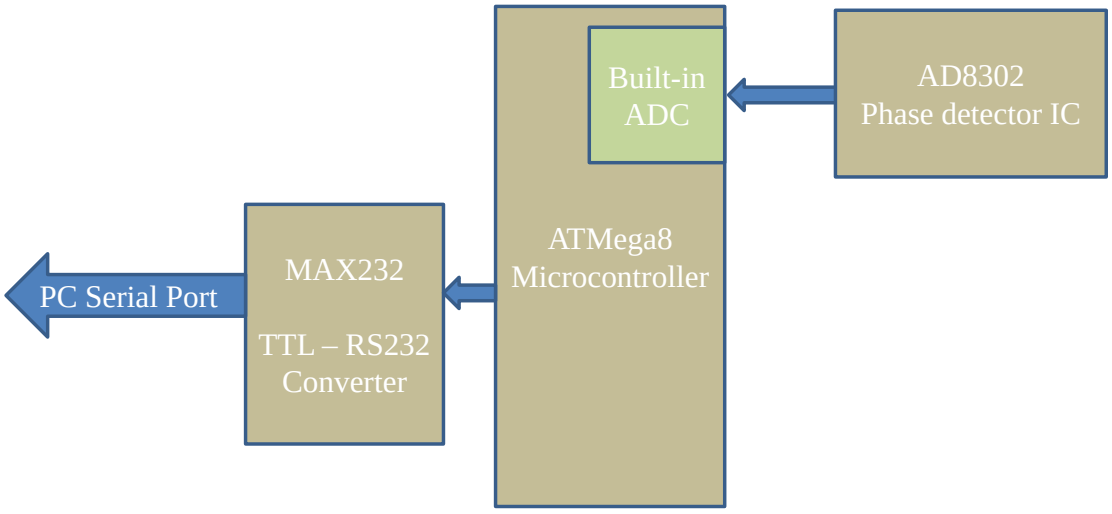

Fig. 2.25: Block diagram of PC Interface circuit.

The ATMega8 microcontroller has a USART (Universal Synchronous and Asynchronous Reception and Transmission) module which can send and receive serial data. The computer has an RS232 serial port which can send and receive serial data. The microcontroller serial data is sent at 0V and 5V digital logic (0V corresponds to logic 0 and 5V corresponds to logic 1). The RS232 serial port of a computer transmits serial data at -13V and +13V digital logic (-13V corresponds to logic 1 and +13V corresponds to logic 0) Hence the microcontroller voltage levels need to be converted to the RS232 voltage levels. An IC called MAX232 is used for the same purpose.

A windows executable was created to access serial data, interpret it and then save in a file. The coding required for this executable was done in Visual C programming environment. A serial transmission data rate of 19200 bits/s is used. This corresponds to a byte rate of 2400 bytes/s. Four bytes comprised of one sample data. Hence, the sampling rate of the LIDAR during the PC interface period is 600 samples/s. As the error rate at this bit rate is relatively high, two start bytes have been used for transmission and error checking. The format of transmission of data from the microcontroller to the computer is

```
';'  '$'  'ADC_lowByte'  'ADC_highByte'
```

in the same order. By checking if the first two bytes match with `';'` and `'$'` the validity of the data can be verified. Only the correct data samples will be saved into the file.

CHAPTER 3

Implementation of System

3.1 Introduction

In chapter 2, the detailed design of each subsystem is shown. In this system, the implementation of each subsystem is shown. This mainly comprises of the pictures of the system and some issues which may have been faced during implementation. Each of the following sections goes through the implementation of the designs discussed in chapter 2 listing out some issues which were faced and their solutions if applicable.

3.2 Implementation of each module

3.2.1 Modulated Laser Transmitter

The Laser transmitter as mentioned earlier was implemented from a Laser pointer diode. Some issues which were faced during the implementation and the solutions found are given below (Round bullets show the issue and tick mark bullets show the solutions)

- **Uncertainty whether the Laser diode was actually getting modulated:** Every Laser diode has a parasitic capacitance inside. As the Laser diode used was not a standard component, it lacked a clear datasheet due to which this capacitance was not known. Hence, even though a modulated input signal was given to the Laser diode it was not known whether the Laser's light output was actually getting modulated.
    - ✓ A Transimpedance amplifier of bandwidth > 50MHz was made and the Laser diode was tested. Making the Transimpedance amplifier with the required bandwidth was the main problem

- **Uncertainty of the voltage levels to be given to the Laser diode:** A Laser diode is very sensitive to the current which flows through it. Current beyond the maximum limit even for a small duration may spoil the diode.
    - ✓ Different diodes were experimented with different voltages and the best modulating voltage was experimentally found out.
- **High power Laser diodes have internal driver circuitry:** As the transmitted light need to be of sufficiently high intensity, a high power laser pointer diode was chosen. This has a problem that unlike the other laser pointers which just have a current limiting resistance in series; these Laser diodes have driver circuitry. These driver circuits are designed for DC operation and cannot respond to modulation at high frequencies.
    - ✓ The driver circuit was bypassed and the modulation signal was directly given through a series resistance. The negative implications of bypassing the driver circuitry are not yet clearly known.

A picture of the Laser diode and the diverting mechanism is shown in Fig. 3.1

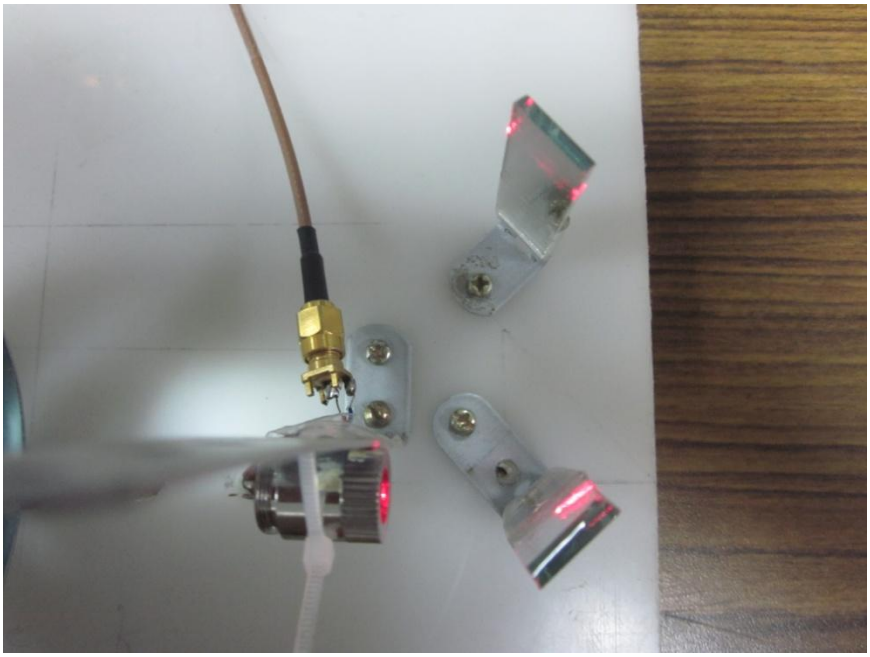

Fig. 3.1 Laser diode and diverting mechanism.

3.2.2 Focusing Mechanism & Diverting Mechanism

The focusing mechanism was implemented with three convex lenses placed co-axially such that their focus falls on the photo-diode. The diverting mechanism was made by placing a partially reflecting mirror and a fully reflecting mirror at 45° to each other. The following are some issues faced during the implementation of both these mechanisms.

- **Alignment of the convex lenses:** As the active area of the photo-diode is very small (about 0.5mm x 0.5mm), it was very difficult to place the photodiode exactly at the focus of the lenses.

    - ✓ The position of the photo-diode was made finely adjustable by providing bolts on which the PCB holding the photo-diode can be mounted and moved. Also, multiple holes were provided for adjusting the position of lenses as required. Above all, careful calculation of focal lengths and image distances and careful fabrication of the board was done to avoid any problems in the first place.

- **Uncertainty in the position of the image:** Because of the dark colour of the inside cavity of the photo-diode, the exact position of the image was unknown when the light is allowed to fall on the photo-diode. i.e. there was an issue knowing whether the focused light was falling on the active region of the photodiode or some other inactive region inside the photo-diode.

    - ✓ Whenever a new alignment was made, a white paper was placed just in front of the photodiode and the position of the object was moved to check if the image was falling at the centre of the photo-diode.

- **Alignment issues in diverting mechanism:** The two mirrors to divert the beam are mounted on two metal L-bends. Careful alignment of these L-bends is required so that the Laser light beam falls exactly on the Photodiode-1 (refer to Fig. 2.1). Due to slowly reacting elasticity of the metal L-bends, the angle of the reflected Laser light changed slowly over time. This resulted in low current signal in Photodiode-1.

- ✓ Repeated trials were made to align the mirrors and once the perfect alignment was made, it was not disturbed.

- **Shadow of the Laser diode on Photodiode:** As both the photo-diode and the Laser diode were placed on the principal axis of the lens, for small target distances, the shadow of the lens covers the active region of the photo-diode.

  - ✓ Using Laser diodes which have inbuilt photo-diodes in them is a solution. This has not been implemented in the present work.

- **Perfectly horizontal arrangement of the Laser diode:** If the Laser is not perfectly aligned with the principal axis of the lens, the position of the centre of the image formed will change with the target distance. This means, that the image might not fall on the active area of the photodiode for most of the target positions. To avoid this, the Laser needs to be aligned with the principal axis of the lenses.

  - ✓ Careful alignment of the Laser diode was made and was not disturbed on done perfectly.

Fig. 3.2 shows the focusing mechanism and the diverting mechanism.

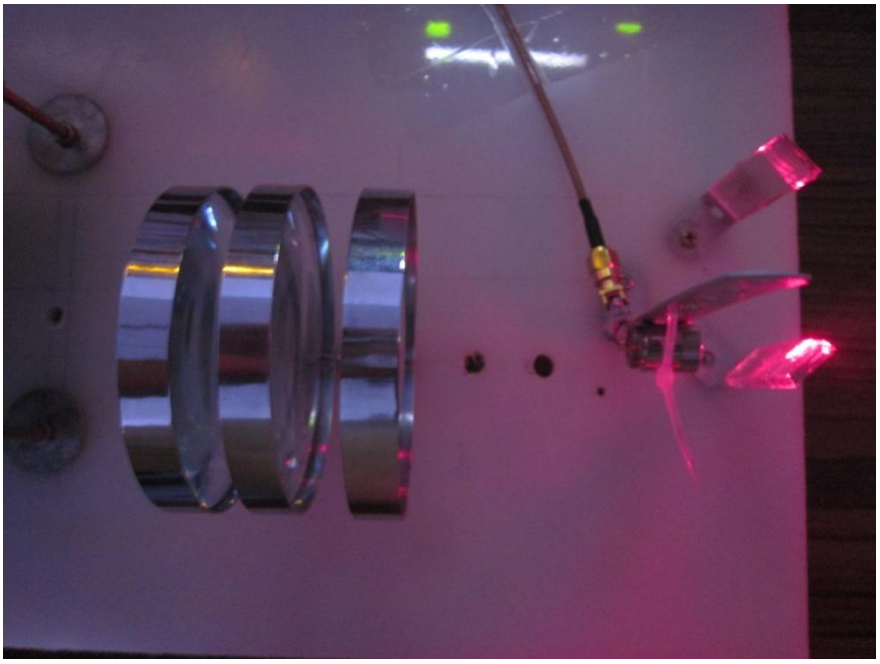

Fig. 3.2 Focusing and diverting mechanisms.

3.2.3 Photodetector circuit

As seen in the earlier chapter, the 'Current sensor + Unity gain buffer' type circuit was chosen as the photo-detector circuit. An inductance of 120nH was chosen. The capacitance of 140pF was realised approximately by putting two 68pF in parallel. There was just one main issue in this stage which is mentioned below.

- **Unwanted coupling:** There was an unwanted coupling at the start of the Photodetector circuit which showed up as a large amplified unwanted signal at the output. This unwanted signal is seen even when zero input is given. The reason for this coupling was not exactly understood.

    - ✓ Covering the Photodiode-2 with an aluminium foil (seen on bottom right corner of Fig. 3.3) such that it is completely isolated from Photodiode-1 solved the problem of the unwanted noise.

A photograph of the photo-detector circuit, amplifier circuit and the phase-detector circuit has been presented in Fig. 3.3.

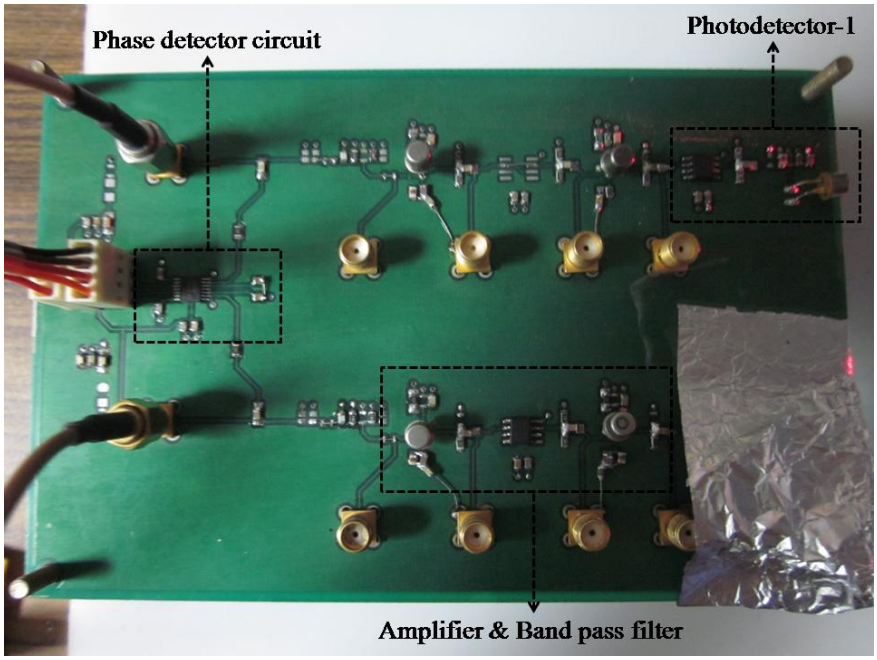

Fig. 3.3: Phase detector circuit, amplifier circuit & photo-detector circuit.

3.2.4 Amplifier & Band pass filter circuit

The implementation of this stage was again quite straight forward. The main issue faced in implementing this stage was as follows:

- **Risk of excessive output signal amplitude:** The stage which succeeds the amplifier circuit is the phase detector circuit. The phase detector can take a signal of maximum amplitude of 0.7V. Any signal larger than this may permanently damage the IC. As the intensity and the gain may differ from the ideally calculated values, it was risky to directly give the amplifier output signal to the phase detector IC.

    - ✓ Suitable attenuation was added to the signal so that the signal seen by the AD8302 IC does not exceed 0.7V for any target distance. The values were measured on an oscilloscope before the IC was connected. Provision for SMD jumpers was made in the PCB to facilitate the same.

- **Large V_{CC} coupled noise:** Due to an error while designing the PCB, provision for local bypass capacitors was not provided for the LC tuned amplifiers. This caused increased noise in the signal

    - ✓ SMD capacitors were soldered using short air wires as bypass capacitors to reduce the noise.

3.2.5 Phase detector circuit

AD8302 IC and the appropriate filter capacitors mentioned in section 2.4.5 were soldered. There were no notable issues with this stage of the circuit.

3.2.6 Distance decoder circuit & PC Interface circuit

Some of the main issues related to the distance decoder circuit were

- **Poorer resolution:** As the microcontroller used has only sufficient number of pins to connect three seven segment displays, the resolution of the distance decoder circuit is 1cm which is poorer than the actual resolution of the LIDAR.

- ✓ This issue has been solved by making the PC interface circuit to directly transfer the data to the computer.

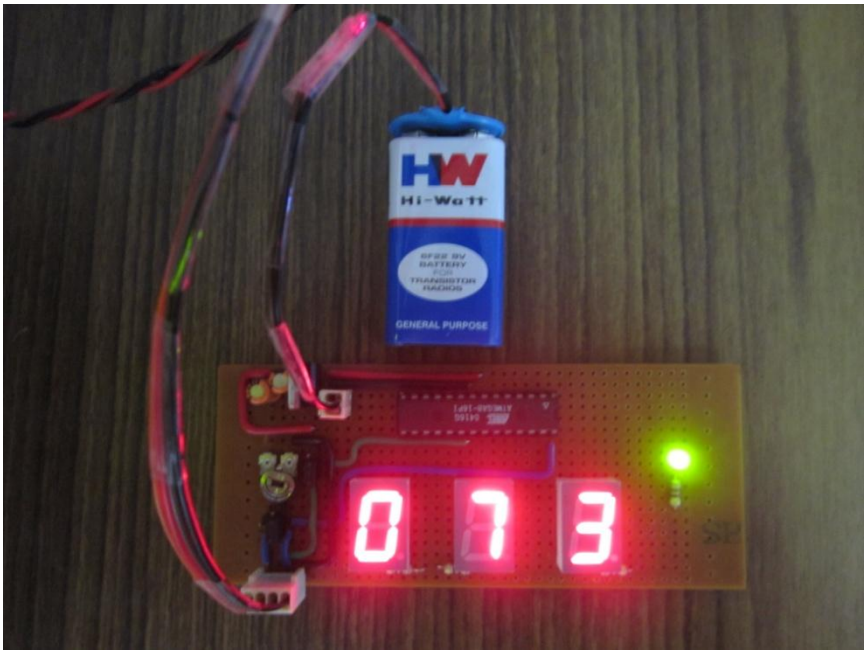

Fig. 3.4: Distance decoder circuit with 73cm as the output on the 7 segment display.

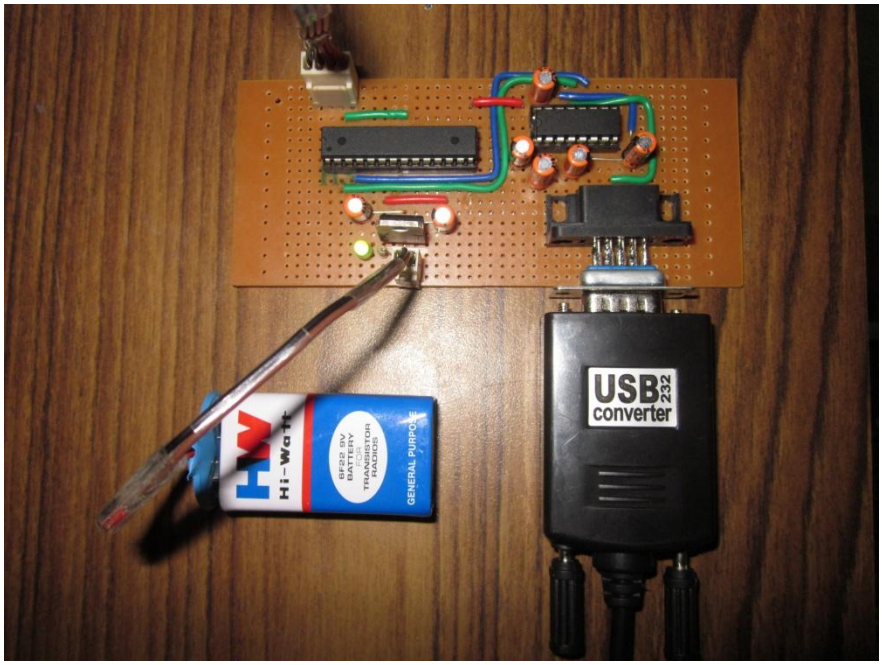

Fig. 3.5: PC Interface circuit.

Fig. 3.4 & 3.5 show the distance decoder circuit and the PC interface circuit respectively.

3.3 System view

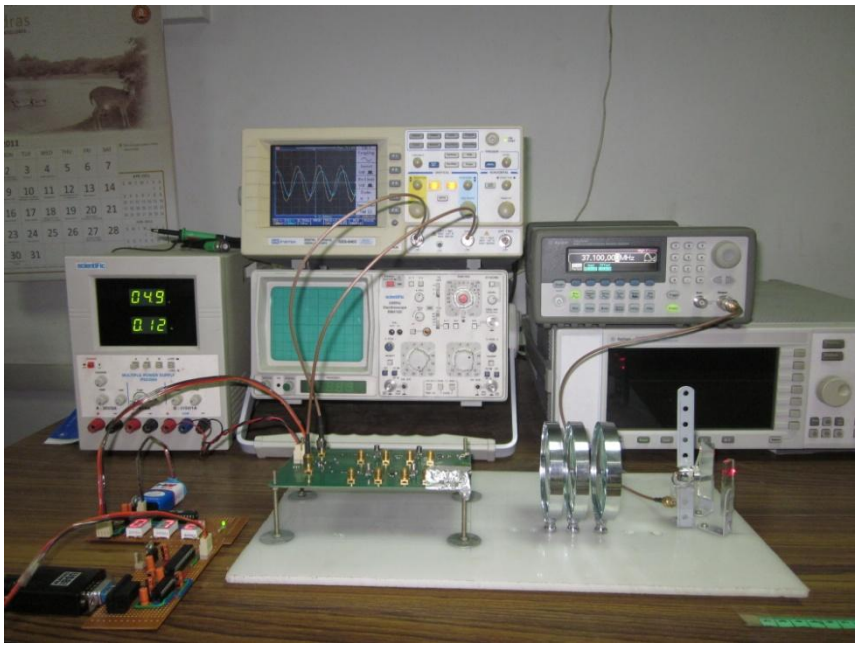

Fig. 3.6: LIDAR setup with testing equipment.

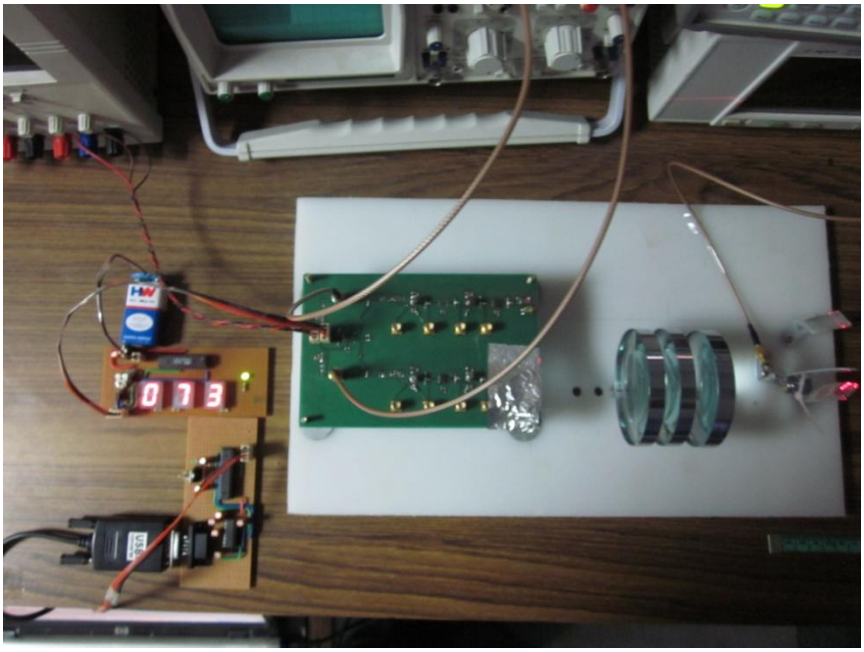

Fig. 3.7: LIDAR setup top view.

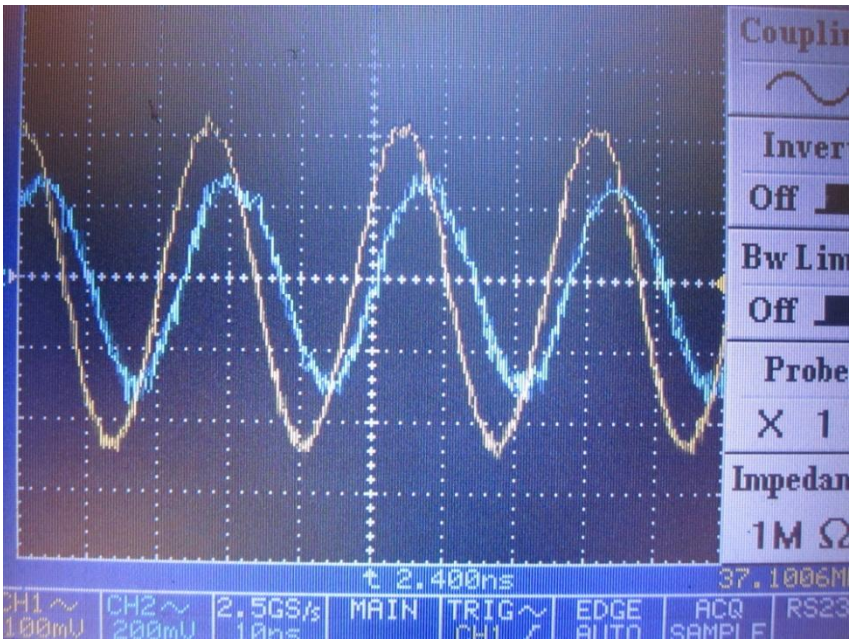

Fig. 3.8: Phase difference between reflected light & reference light

In the above figure, yellow signal corresponds to reference light and blue signal corresponds to reflected light.

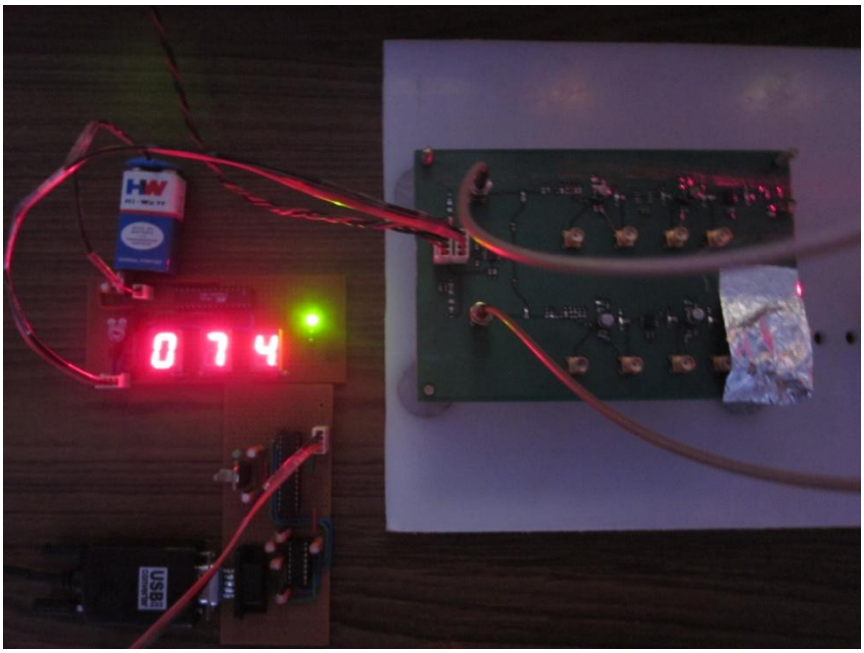

Fig. 3.9: Receiver circuit, distance decoder circuit and PC Interface circuit.

CHAPTER 4

Results & Discussion

4.1 Video

A working video of the Laser range finder built in this project can be found at the link: http://www.youtube.com/watch?v=yjsqrlKow44 . A detailed explanation of how the system works and a demonstration is given in the above link.

4.2 Comparison of measured distance with actual distance

Fig. 4.1 shows the Measured distance vs. Actual distance graph.

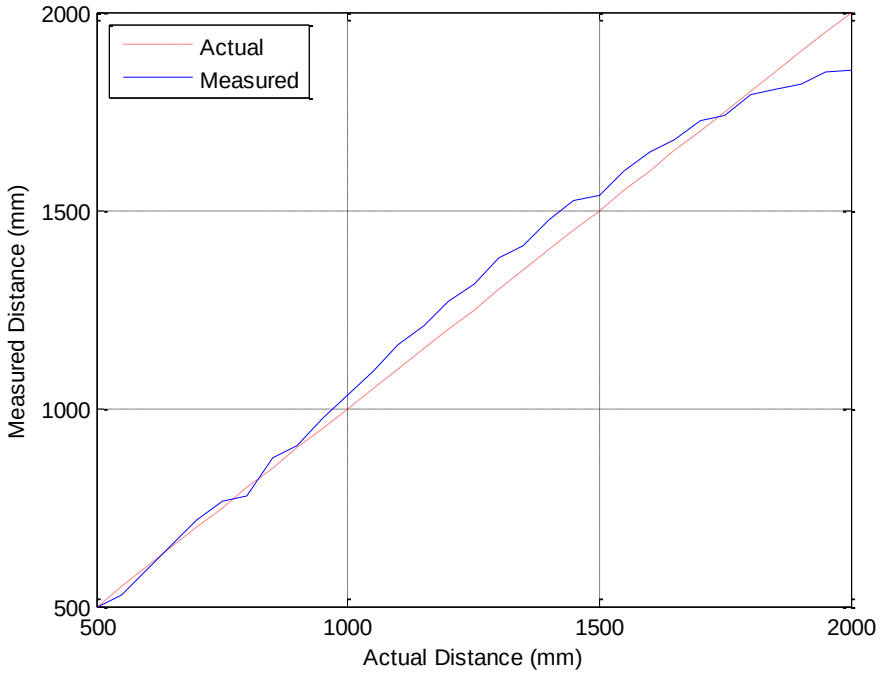

Fig. 4.1: Measure distance vs. Actual distance

As it can be seen, the measured distance is always greater than the actual distance for most of the readings. Also, the error is lesser than 6% between 50cm and 1.8m. Till about 1.5m, the measured distance is almost linear and hence a change in the scaling factor can

fix the issue. But the reason that 6% erroneous measurements are being made can be any of the following reasons:

- **Nonlinearity in Phase detector:** The voltage levels being given to the phase detector at the minimum target position (i.e. 50cm) are about the maximum that can be given to the phase detector IC. Due to this there might be some nonlinear scaling coming up in between the distance and the output voltage.

- **Residual signal:** When no input is being given to the receiver there can be small residual signal that can be seen. This may be due to some pick up from the environment. The amplitude of this signal is about 10mV. Hence, for higher distances, the measurement becomes more and more inaccurate.

The actual distance vs. error graph can be seen in Fig. 4.2

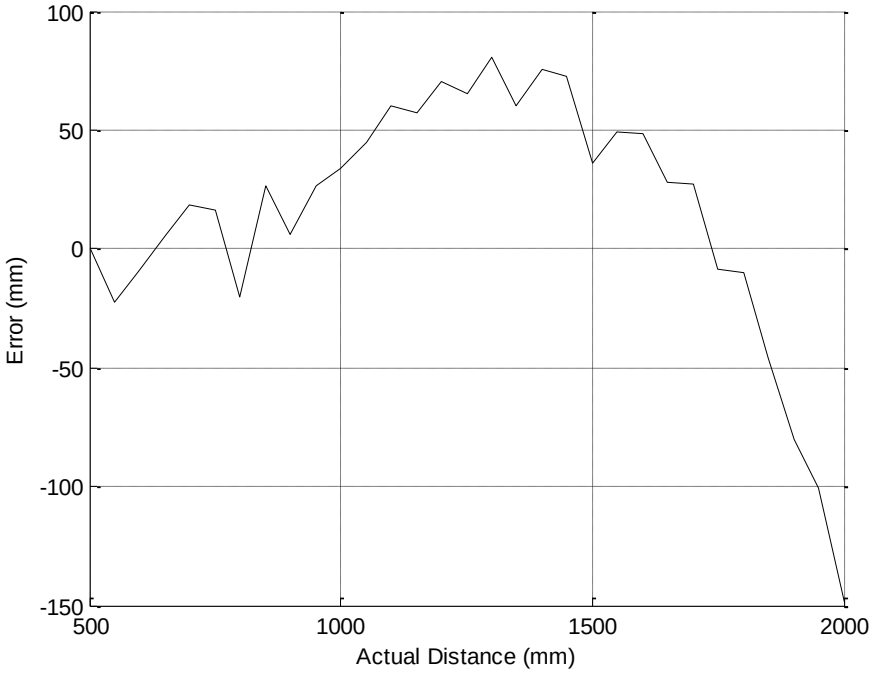

Fig. 4.2: Error vs. Actual distance

Fig. 4.3 shows the percentage error vs. Actual distance. It can be seen that till about 1.9m, the percentage error is less than 6%.

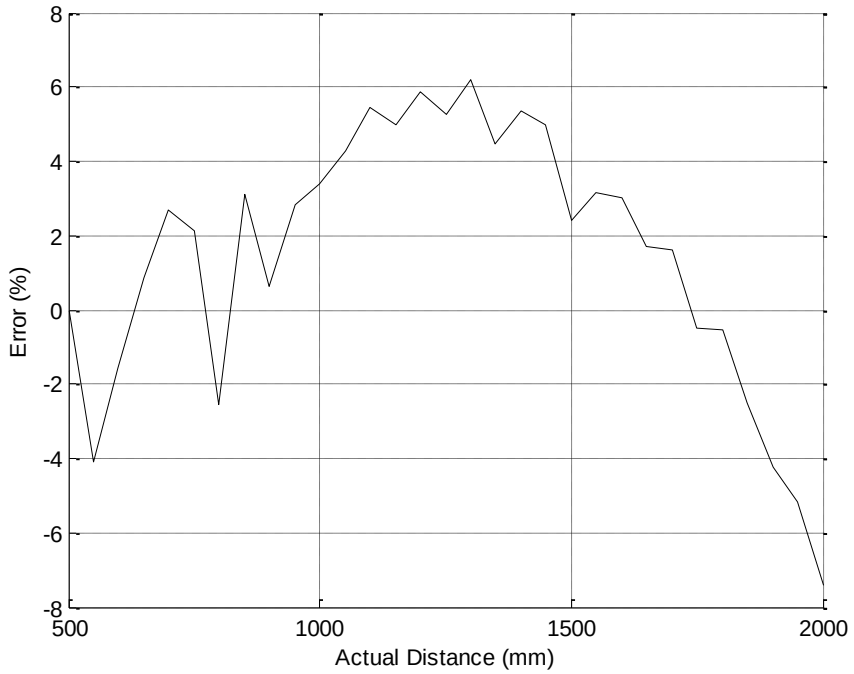

Fig. 4.3: Percentage error vs. Actual distance

4.3 Standard deviation of the measured distance

At a target distance of 750mm, LIDAR readings were taken continuously for 10 minutes. The mean of the data over the 10minutes comes to 753mm while the standard deviation of the data comes to 5.6mm.

At a target distance of 1500mm, LIDAR readings were taken continuously for 10 minutes. The mean of the data over 10 minutes comes to 153.5mm while the standard deviation of the data comes to 2mm.

The above values show that averaging over long time, though the mean value may not be very close to the actual value, the variance of the measured value is small. This means that the LIDAR has better precision and needs to be improved in terms of accuracy.

4.4 Percentage error vs. Actual distance graph for different colours

Figures, Fig. 4.4, Fig. 4.5, Fig. 4.6, and Fig. 4.7 show the error vs. Actual distance graphs for mild blue, mild green, pink and yellow screens respectively..

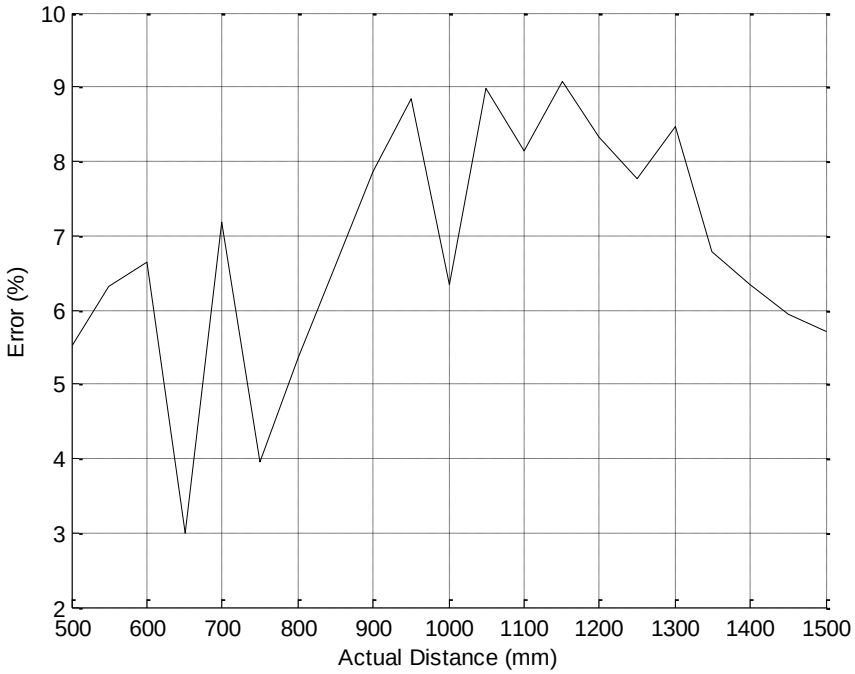

Fig. 4.4: Percentage error vs. Actual distance for mild blue screen

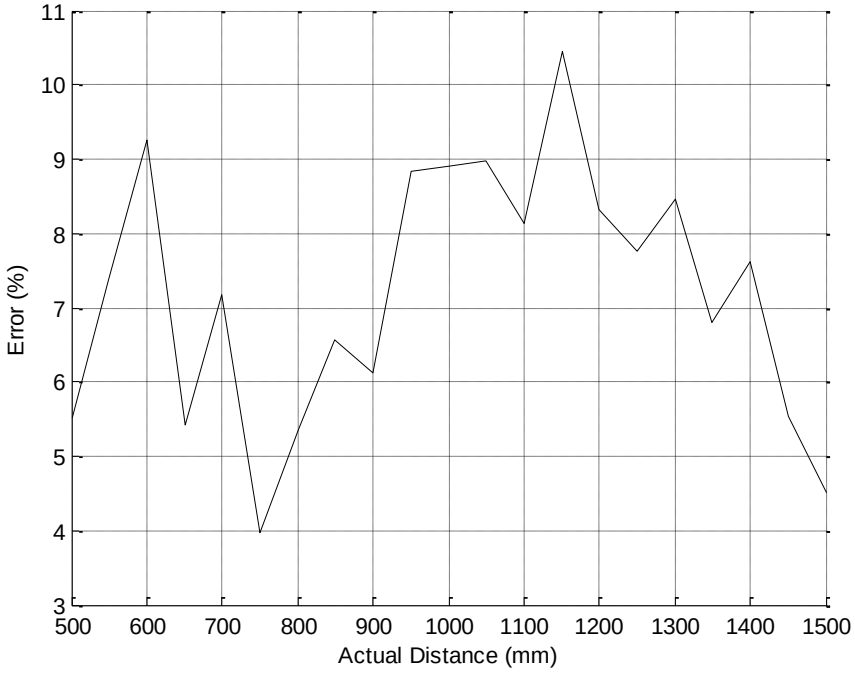

Fig. 4.5: Percentage error vs. Actual distance for mild green screen

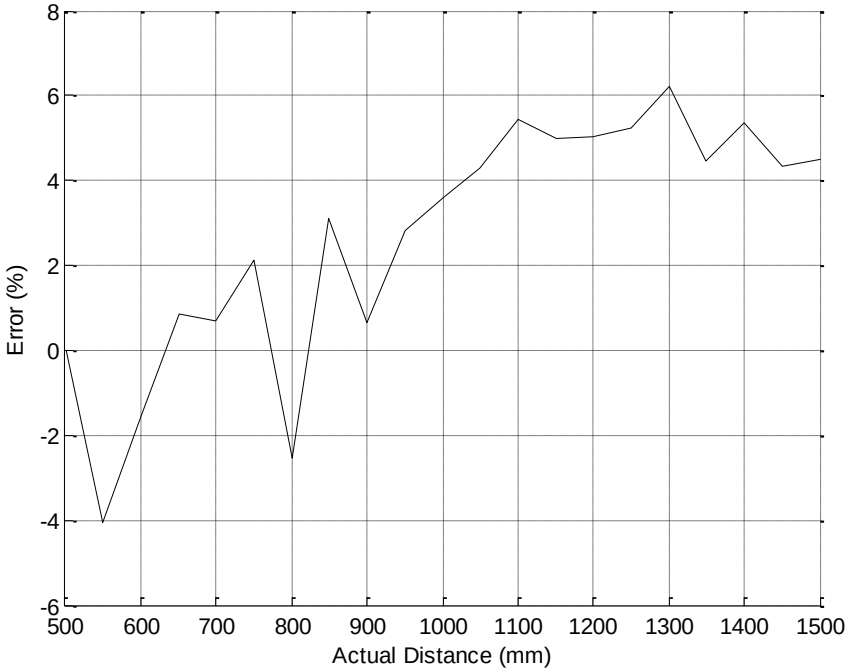

Fig. 4.6: Percentage error vs. Actual distance for pink screen

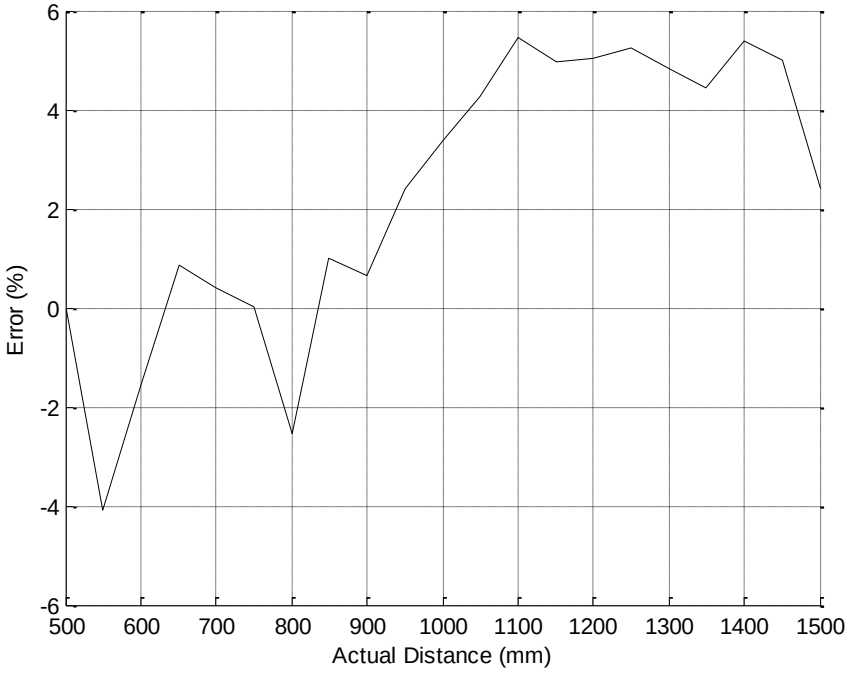

Fig. 4.5: Percentage error vs. Actual distance for yellow screen

As expected, the LIDAR performs poorer with the colours which do not have red colour in them, like blue and green. Yellow and pink, which have a component of red colour in them, reflect red light better and hence, the LIDAR performs better with them.

CHAPTER 5

Conclusions and future work

5.1 Conclusions

In this project, a system level design and implementation of a phase difference type Laser range finder has been presented. An intensity modulated Laser light is sent to the target. The light reflected from the target is detected using a photodiode and amplifier circuit. The phase difference between the transmitted light and the received light is directly proportional to the distance. This phase difference is measured and the distance is estimated. This distance is shown on a display in units of centimeter. The data can also be logged on a computer.

The design is implemented on a Printed Circuit board. The Laser Range finder made has a range of 0.5m to 1.8m and a resolution of 2mm. It can update the distance onto a computer at a rate of 600 samples per second. The accuracy of the Laser Range finder has been tested for white surfaces. The measured data, standard deviation of the measured data, accuracy and other parameters have been presented. A video of the LIDAR has been uploaded on YouTube at http://www.youtube.com/watch?v=yjsqrlKow44.

5.2 Future work

As the magnitude of the signal is the main problem behind all these, using a more sensitive photo-diode will solve many problems. An Avalanche Photodiode if used can increase the sensitivity by about 2 orders of magnitude. The drawback is that an Avalanche photodiode requires high DC bias voltage of about 100V which needs to be supplied to it.

Another improvement which can be made is that a Q switched Laser diode can be used. The Laser diode being used presently is a continuous wave diode, i.e. it emits light

continuously. Instead, there are Laser diodes which can emit high powers for small bursts of time and thus keep the average power low but the signal magnitude high. Usage of these Laser diodes can be another improvement which can be made.

Reduction of size is also possible by the use of both the above techniques and the present LIDAR can be improvised to make a scanning Laser range finder

REFERENCES

1. "Surveying for Engineers - 4th Edition" by J. Uren & W.F. Price.
2. "Development of Ultra-Small Lightweight Optical Range Sensor System" by Hirohiko Kawata, Akihisa Ohya & Shin'ichi Yuta from University of Tsukuba and Santosh Wagle & Toshihiro Mori from Hokuyo Automatic Co., Ltd.
3. "Frequency Response of Common Transistor Amplifiers" by Prof. Michael Tse. Available as online course material at http://cktse.eie.polyu.edu.hk/eie304.
4. A block diagram of a Laser Range finder given in the following website : http://www.element14.com/community/docs/DOC-22620/l/block-diagram--laser-rangefinder-solution.
5. "Fundamentals of Photonics" by Baaha E A Saleh & Malvin Carl Teich.
6. "Microelectronic Circuits – 5th Edition" by Sedra & Smith.
7. Wikipedia pages of LIDAR, Common Emitter amplifier, Common collector amplifier & Common base amplifier.